AD-A007 785

CONTROLLABLE LIQUID ARTIFICIAL DIELECTRIC S-BAND PHASE SHIFTERS

S. Mikuteit, et al

General Dynamics

Prepared for:

Rome Air Development Center

February 1975

DISCLAIMER NOTICE

THIS DOCUMENT IS BEST QUALITY PRACTICABLE. THE COPY FURNISHED TO DTIC CONTAINED A SIGNIFICANT NUMBER OF PAGES WHICH DO NOT REPRODUCE LEGIBLY.

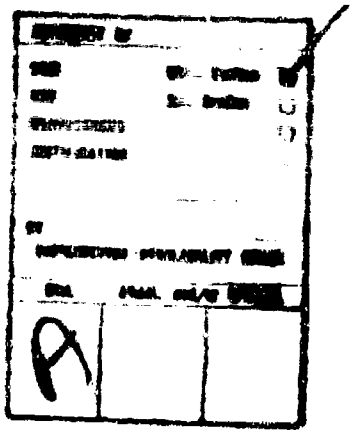

UNCLASSIFIED
SECURITY CLASSIFICATION OF THIS PAGE (When Data Entered)

REPORT DOCUMENTATION PAGE	READ INSTRUCTIONS BEFORE COMPLETING FORM
1 REPORT NUMBER: RADC-TR-75-21	2 GOVT ACCESSION NO. / 3 RECIPIENT'S CATALOG NUMBER
4 TITLE (and Subtitle): CONTROLLABLE LIQUID ARTIFICIAL DIELECTRIC S-BAND PHASE SHIFTERS	5 TYPE OF REPORT & PERIOD COVERED: Final Technical Report 18 Jun 73 to 18 Jun 74
	6 PERFORMING ORG. REPORT NUMBER: A-74-59
7 AUTHOR(s): S. Mikuteit, W. Bottenberg	8 CONTRACT OR GRANT NUMBER(s): F30602-73-C-0325
9 PERFORMING ORGANIZATION NAME AND ADDRESS: General Dynamics/Electronics Division, P O Box 81127, San Diego CA 92138	10 PROGRAM ELEMENT, PROJECT, TASK AREA & WORK UNIT NUMBERS: 01707307
11 CONTROLLING OFFICE NAME AND ADDRESS: Rome Air Development Center (OCTE), Griffiss AFB NY 13441	12 REPORT DATE: February 1975
	13 NUMBER OF PAGES: 47
14 MONITORING AGENCY NAME & ADDRESS (if different from Controlling Office): Same	15 SECURITY CLASS (of this report): UNCLASSIFIED
	15a DECLASSIFICATION/DOWNGRADING SCHEDULE: NA

16 DISTRIBUTION STATEMENT (of this Report)

Approved for public release; distribution unlimited.

17 DISTRIBUTION STATEMENT (of the abstract entered in Block 20, if different from Report)

Same

18 SUPPLEMENTARY NOTES

RADC Project Engineer:
Joseph M. Schemna (OCTE)
Griffiss AFB NY 13441
AC 315 330-4251

The effort described in this report was funded in part with the Laboratory Director's Discretionary Funds.

19 KEY WORDS (Continue on reverse side if necessary and identify by block number)

Phase shifters, microwave	Liquid crystals
Waveguide transmission line	Protein solutions
Liquid dielectrics	Ferrofluidics
Metallic suspensions	Surfactants

20 ABSTRACT (Continue on reverse side if necessary and identify by block number)

This report describes the work done to prove the feasibility of developing a new class of microwave phase shifters based on the concept of electrically controllable liquid artificial dielectrics using metallic suspension. The theory of operation shows the explicit relationship between material parameters and device performance characteristics. A new electrode design configuration is described that reduces insertion loss characteristics. Result show that particle agitation is not required. Test data of metallic

(Cont'd)

DD FORM 1 JAN 73 1473 EDITION OF 1 NOV 65 IS OBSOLETE

UNCLASSIFIED
SECURITY CLASSIFICATION OF THIS PAGE (When Data Entered)

20. Abstract (cont'd.)

suspensions, liquid crystals, and certain proteins are given. Test data are given for insertion loss characteristics, VSWR, and phase shift as a function of applied voltage over the band of frequencies from 2.7 to 2.9 GHz.

The prospects for new material compositions are discussed as well as their relative merits. Recommendations are made for further studies. Important new findings on particle agitation and the use of surfactants amending previously held beliefs are documented.

CONTROLLABLE LIQUID ARTIFICAL DIELECTRIC S-BAND PHASE SHIFTERS

S. Mikuteit
W. Bottenberg

LDP No. 01707307

PREFACE

This Final Report describes work performed by the General Dynamics/ Electronics Division, San Diego CA 92138, under Contract F30602-73-C-0325, Job Order 01707307, for Rome Air Development Center, Griffiss Air Force Base, New York. The report covers work performed from June 1973 to June 1974.

The RADC Project Engineer is Joseph M. Schenna (OCTE).

The authors are greatly indebted to R. P. McNamara now on leave of absence to the University for conducting all work on phase shifter design, low power testing and his contribution to the paper; to C. Meierbachtol and D. Conshor for establishing the high power S-band laboratory and conducting the high power phase shifter tests; and to E. O. Mayfield for reviewing the manuscript.

The effort described in this report was funded in part with the Laboratory Director's Discretionary Funds.

This report has been reviewed by the RADC Information Office (OI) and is releasable to the National Technical Information Service (NTIS). At NTIS it will be available to the general public, including foreign nations.

This technical report has been reviewed and is approved for publication.

APPROVED: Joseph M. Schenna

JOSEPH M. SCHENNA
Project Engineer

APPROVED: William T. Pope

WILLIAM T. POPE
Assistant Chief
Surveillance Division

FOR THE COMMANDER: James G. McGinnis

JAMES G. McGINNIS, Lt Col, USAF
Deputy Chief, Plans Office

OBJECTIVE OF CONTRACT

The objective of this contract is to demonstrate the feasibility of developing a new class of microwave waveguide phase shifters based on the operating concept of electronically controllable liquid artificial dielectrics. The study is to be directed toward analog, reciprocal devices that are simple in construction, can be produced at low cost in small quantities, can handle high power levels, and have an insertion loss of less than 2 dB for 360° phase shift. The phase shifters are to operate at S-band frequencies, handle peak power levels of greater than 1.25 megawatts, and an average power level of up to 5 kilowatts. An essential factor in the program is a chemical/physical structure study of dielectric materials that represents the best trade-off in terms of performance and reproducibility.

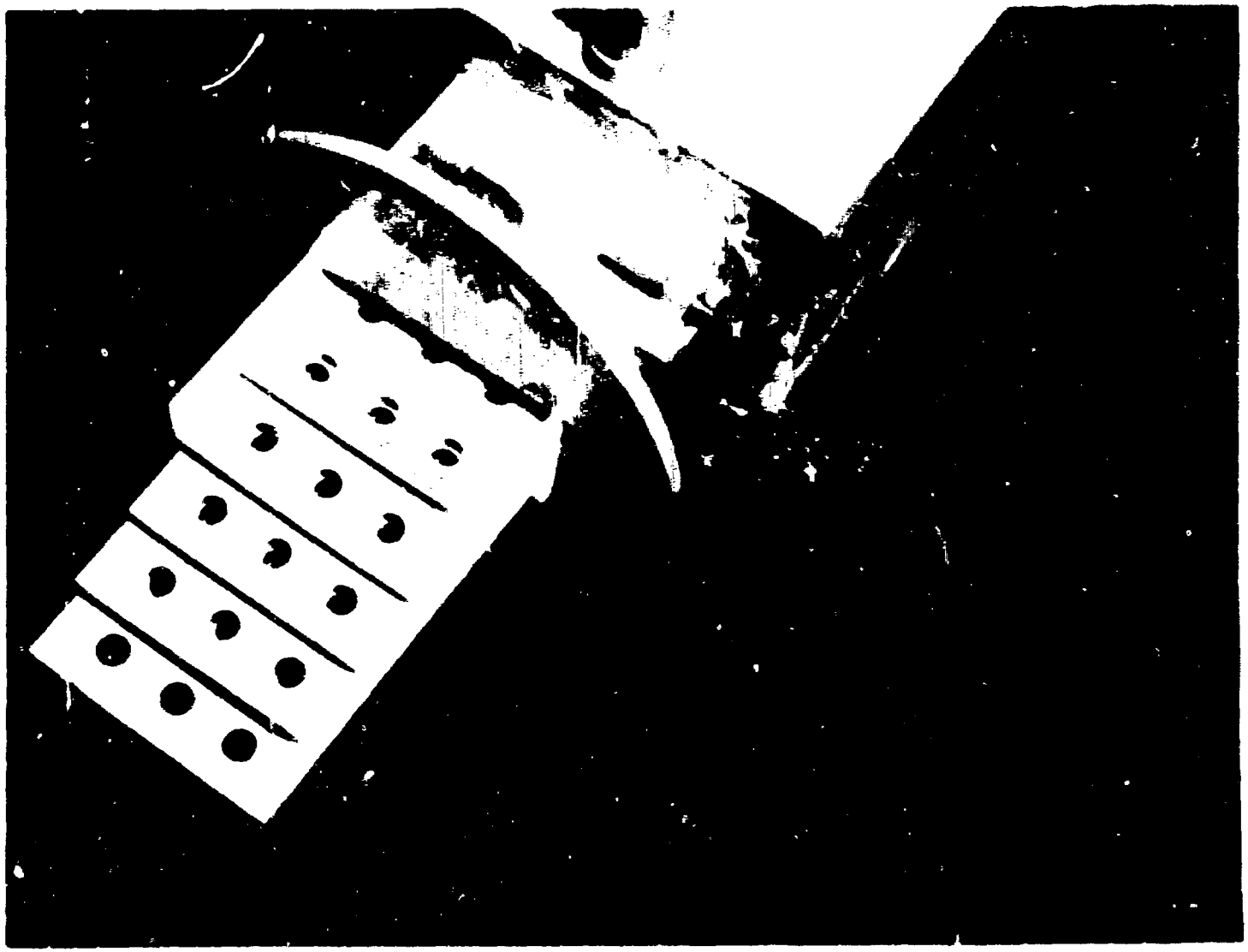

Frontispiece

CONTENTS

Section			Page
	ABSTRACT		xi
1	INTRODUCTION		1
2	THEORETICAL CONSIDERATIONS		3
	2.1	Physical Considerations	3
	2.2	Kerr Effect	3
	2.3	Artificial Dielectric	7
	2.4	The Kerr Effect of Metallic Suspensions	8
	2.4.1	Kerr Effect Magnitude	8
	2.4.2	Response Time and Relaxation Phenomena	18
3	ELECTRODE DESIGN		23
	3.1	Design Goals	23
	3.2	Design Reduction of Control Voltage	23
	3.3	Design Reduction of Insertion Loss and VSWR	26
	3.4	Insertion Loss vs. Phase Shift	31
	3.5	Electrode Fabrication	33
4	PUMPING SYSTEM		35
	4.1	General Design	35
	4.2	Particle Settling and Flow Birefringence (Maxwell Effect)	36
	4.3	Temperature Control	38
5	MATERIALS AND MATERIAL PROPERTIES		39
	5.1	General Considerations of Mechanical and Chemical Stability	39
	5.2	General Considerations of Phase Shifting Requirements	41
	5.3	Metal Particulate Systems	41
	5.3.1	Source of Phase Shift Characteristics	41
	5.3.2	Current Capabilities	41
	5.3.3	System Description	42
	5.3.4	Method of Manufacture	42
	5.3.5	Prospects	43

CONTENTS (Continued)

Section			Page
	5.4	Liquid Crystal Systems	44
	5.4.1	Source of Possible Phase Shift Characteristic	44
	5.4.2	Current Capabilities and Results	44
	5.4.3	Problem Areas and Prospects	44
	5.5	Ferro-Fluid Systems	45
	5.5.1	Source of Phase Shifting Characteristics	45
	5.5.2	Prospects	46
	5.6	Protein Solution Systems	46
	5.6.1	Source of Phase Shifting Characteristics	46
	5.6.2	Prospects	46
6	PERMITTIVITY TESTS		49
	6.1	Dielectric Test Cell	49
	6.2	Cell Construction and Test Set Up	49
	6.3	Permittivity vs. Concentration	49
	6.4	Long Term D.C. Voltage Effects	50
7	LOW POWER TESTING		53
	7.1	Insertion Loss, Electrode Design	53
	7.2	VSWR, Electrode Design	57
	7.3	Phase Shift vs. Control Voltage	58
	7.3.1	Electrode Configuration	58
	7.3.2	Al-CCl_4 Materials Testing	62
	7.3.3	Mg-CCl_4 Materials Testing	63
	7.3.4	Dispersion of Phase Shift	65
8	HIGH POWER TESTS		67
9	SUMMARY AND CONCLUSIONS		77
10	BIBLIOGRAPHY		81

ILLUSTRATIONS

Figure	Title	Page
2-1	Kerr Effect	4
2-2	Views of Prolate and Oblate Spheroids	8
2-3	Orientation Angles for Ellipsoids in a Bias Field	9
2-4	Depolarization Ratio Dependence (A) on Shape Ratio (δ)	12
2-5	Depolarization Ratio Dependence (A) on Shape Ratio (δ) in the Disc-Like Region	13
2-6	Anisotropy Shape Factor (Q) Dependence on Shape Ratio (δ)	13
2-7	Square of Shape Factor (Q) Dependence on Shape Ratio (δ)	14
2-8	Dependence of Orientation Factor (ϕ) on Boltzman Factor (γ)	15
2-9	Effective Specific Kerr Constant Against Volume Fractions of Second Component	17
2-10	Switched-on and Switched-off Behavior of Permittivity Difference ($\Delta\epsilon'$) in the Low-Field Case	19
2-11	Logarithmic Plot of Response Time (τ_F) vs. Particle Size (ℓ) for Different Values of Shape Factor (Q')	20
3-1	S-band Phase Shifter Fabricated Using K_u Band Version	24
3-2	Initial S-Band Phase Shifter Performance	25
3-3	Phase Shifter with Pentaplate Electrode Configuration	27
3-4	Comparison of Phase Shift Obtained for Single and Pentaplate Configurations	23
3-5	Insertion Loss Peaks Caused by Generation of Higher Order Modes	28
3-6	Computer Derived Mode Distribution Using Measured Amplitude Distribution Across Waveguide Width	29
3-7	Insertion Loss Change as a Function of Mismatch Caused by Changing Permittivity	32
3-8	Boundary Region Between Phase Shift Cell and Air-Filled Waveguide	33
4-1	Flow System Schematic for K_U-Band Cell	35
4-2	Velocity Profile of Liquid Flow Between Two Parallel Plates	36
4-3	Phase Shifter Cell with Cooling Fins	38
6-1	Capacitance Test Cell to Measure Permittivity With Changes in Applied Voltage	50
6-2	Change in Permittivity for Various Particle Loading Densities of Silberline "AA" Aluminum	51
6-3	Change in Permittivity for Two Particle Loading Densities of Magnesium Powder, Reade 325-X	51
6-4	High Field Strength Overshoot in Permittivity Change vs. Time for Particle Densities Greater than 20 mg/cc	52

ILLUSTRATIONS (Continued)

Figure	Title	Page
7-1	Insertion Loss Test Setup	53
7-2	Insertion Loss vs. Frequency for Single Electrode Phase Shifter for Various Hole Sizes with CCl_4	54
7-3	Insertion Loss vs. Frequency for Phase Shift Cell Without Electrode and Filled with Carbon Tetrachloride	55
7-4	Insertion Loss for Pentaplate Electrode with Carbon Tetrachloride	56
7-5	Insertion Loss of Complete Pentaplate Phase Shifter with CCl_4 and Al	56
7-6	VSWR Test Setup	57
7-7	VSWR vs. Frequency for Phase Shift Cell Without Electrode and Filled with Carbon Tetrachloride	58
7-8	VSWR vs. Frequency for Single Electrode Phase Shifter for Various Hole Sizes	59
7-9	VSWR of Pentaplate Electrode with Carbon Tetrachloride	60
7-10	Phase Shift Measurements Test Setup	60
7-11	Phase Shift vs. Applied Voltage with Silberline "AA" Aluminum in Cell	61
7-12	Obtainable Phase Shift with Silberline Powder and Reynolds Paste Aluminum at S-Band	62
7-13	K_u-Band Phase Shift with Various Densities of Silberline "AA"	63
7-14	Phase Shift vs. Applied Voltage for Mg-CCl_4-CBr_4 Dielectric at Various Frequencies and Densities	64
7-15	Phase Shift vs. Applied Voltage Showing Effect of Phase Shift Dependence on Frequency	65
8-1	Test Setup for High Power Liquid Phase Shifter	68
8-2	Insertion Loss vs. Average RF Power Level at Insertion Phase Delay with No Bias Field	71
8-3	Phase Shift vs. Applied Voltage for Various Power Levels	72
8-4	Phase Shifter Cell Electrode Breakdown Caused by Insufficient Electrode Coating	73
8-5	Phase Shift vs Applied Voltage for Various Power Levels After Adding Tergitol	74
8-6	Increase of Phase Shift After Surfactant added to Dielectric	74
8-7	Change of Insertion Loss as a Function of Phase Shift	75
8-8	Relative Phase Shift vs. Power Level at Insertion Phase Delay	75

TABLES

Number	Title	Page
5-1	Metal Particulate System Capabilities at S-Band	42
5-2	Currently Used Metal Particles	43
5-3	Liquid Crystal Systems	45
5-4	Measured Insertion Losses for Some Solvents at K_u-Band	47
5-5	Loss Tangents for Some Solvents at 10 GHz	47
5-6	Some Proposed Phase Shifting Protein Systems	47
8-1	Harmonic Filter Operating Characteristics as a Function of Peakpower Level	70
8-2	Al-CCl_4 Phase Shift Tests	76

ABSTRACT

This report describes the work done to prove the feasibility of developing a new class of microwave phase shifters based on the concept of electrically controllable liquid artificial dielectrics using metallic suspension. The theory of operation shows the explicit relationship between material parameters and device performance characteristics. A new electrode design configuration is described that reduces insertion loss characteristics. Results show that particle agitation is not required. Test data of metallic suspensions, liquid crystals, and certain proteins are given. Test data are given for insertion loss characteristics, VSWR, and phase shift as a function of applied voltage over the band of frequencies from 2.7 to 2.9 GHz.

The prospects for new material compositions are discussed as well as their relative merits. Recommendations are made for further studies. Important new findings on particle agitation and the use of surfactants amending previously held beliefs are documented.

EVALUATION

Project No.: 01707307/450e0903
Contract No.: F30602-73-C-0325
Effort Title: Variable Permittivity Liquid Phase Shifters
Contractor: General Dynamics, Electronics Division, San Diego, CA 92138

1. The purpose of this effort was to determine the feasibility of developing a reciprocal, high power, liquid dielectric, analog phase shifter for operation in the S-band region of the microwave spectrum. As identified in the RADC Technology Plan (TPO-5), these moderate-to-high power electronically controlled phase shifters are currently needed to provide the necessary phase increments to achieve a polarization diversity capability in an existing air traffic control system and in a planned airport surveillance radar, the AN/GPN-12 and -12A, respectively.

2. The effort has advanced the knowledge, design, synthesis and functional operation of a new class of reciprocal microwave phase shifter. In addition, the program has contributed to a long-term overall objective to develop and apply the technology necessary to synthesize any practical liquid dielectric medium featuring electronically controlled permittivity for use in low cost, large bandwidth phase shifting configurations at both low and high power levels at any microwave frequency.

3. The feasibility of the approach was empirically shown in most major goal areas except that of phase-set response time. A newly developed theory, verified by preliminary measurements, predicts that this problem can be solved. Since this and other pertinent microwave characteristics were not resolved or ascertained during the course of this program, a follow-on effort will be necessary in order to determine all the attributes of this potentially promising, phase shifting technique. The continuation of this program not only offers a possible solution to the high power variable phaser dilemma, but could form the basis for a wide range of designs and transmission line applications which would be simple in construction and low cost in both small and large quantity productions. Successful completion of these efforts would advance system capabilities in the areas of long range detection, surveillance and ground control intercept systems, weather detection and penetration aid radars, air traffic control and navigational radar systems.

JOSEPH V. SCHENNA
Project Engineer

I. INTRODUCTION

Phase shifters capable of operating at very high power levels with low insertion loss characteristics and providing reciprocal, analog operation at low cost are currently needed for use on a variety of medium, long range, and other surveillance radars to satisfy such requirements as:

- Warning and Control
- Anti-Submarine Warfare
- Reconnaissance
- Meteorological

They are needed to provide the capability to operate these radars with polarization agility. In addition, high power phase shifters are required for new, cost-effective antenna systems that will be based on the limited-scan concept in which large reflectors utilize high power array feeds capable of amplitude and phase control at each feed element thereby providing considerably extended electronic scanning over that available with phase control only and at high power levels.

At present, two primary types of phase shifters exist — the PIN diode and the Ferrite phase shifters. Neither the diode nor the ferrite phase shifter have attained very high peak and average power handling capability.

The results presented in this report are based on work which deliberately bypassed conventional phase shifter technology. The areas of electro-optics, plasma-physics, and physical chemistry were searched for physical phenomona that might be used as operating principles for a new microwave phase shifter. The most promising approach was synthesized from work done in each of these disciplines.

The result of this work is an electrically controllable artificial dielectric material comprised of metallic particles suspended in a suitable liquid with the suspension exhibiting controllable anisotropy. Variable phase shift is realized by inserting this liquid dielectric in the signal path be it a waveguide or a dielectric lens. Since propagation velocity in dielectrics is inversely proportional to the dielectric constant, changing the effective dielectric constant changes the apparent path length. The permittivity is controlled by applying a low frequency, variable intensity electric field.

This report describes the S-band study of the new phase shifter technique to prove feasibility of the principle of operation, the specific approach chosen, and finally the device itself.

The work carried out on this program and covered in this report was concentrated in five areas.

- **Analytical studies of phase shifter cell design and establishing the theoretical background for determining the relationship between certain device specifications and material parameters. For example response time as a function of particle size and applied field.**
- **Electrode design and eliminating possible moding problems.**
- **Development of a suitable pumping scheme to prevent particle settling. The results obtained are a breakthrough in the sense that it was possible to show that pumping is not at all desired thereby significantly extending operational know-how of this new phase shifter technique.**
- **Material and material properties, among them metallic suspensions, liquid crystals, and also proteins.**
- **Testing the experimental model built at low and high power levels. All of the theoretical and experimental exploration of phase shifter performance parameters are documented in this report by comprehensive data curves.**

2. THEORETICAL CONSIDERATIONS

2.1 PHYSICAL CONSIDERATIONS

When dielectric materials with electronically variable anistropic permittivity are inserted in a microwave signal path, the propagation velocity of the microwave signal is electronically controlled. Hence, a phase shift or phase delay is observed. The dielectric medium may contain conductive particles suspended in a dispersion. Without an external force, the particles exhibit a random orientation due to the agitation of the Brownian movement or thermal motion that normally renders the medium isotropic. When an electric field $\vec{E}$ is applied to the medium, the particles polarize and tend to align their longest axis with the applied field. The medium becomes anisotropic and the Kerr effect is observed.[1]* The degree of statistical alignment and, therefore, the change in permittivity is related to the strength of the control field. The dielectric material displays an electronically variable anistropic permittivity. An anisotropic dielectric is a nonconducting medium whose properties are different in different directions.

2.2 KERR EFFECT

The Kerr effect was first observed with experiments on the optical properties of a medium that was in an applied electric field. The Kerr cell, shown in Figure 2-1 illustrates the phenomenon. When linearly polarized light enters a slab of material that has an applied field $\vec{E}$, the altered refractive index of the medium caused by the applied field will result in an elliptically polarized light beam leaving the cell. The vector of the incident light $\vec{E}_i$, may be resolved into two components, one parallel to the direction of the applied electric field, $E_{\parallel}$, and the other perpendicular to the direction of the applied electric field, $E_{\perp}$. Under the influence of the external field the medium will have refractive indexes ($n_{\parallel} > n_{\perp}$) that are different for each component. Hence, the two components will traverse the medium at different velocities and emerge out of phase.

Without an applied electric field the particles are oriented at random. The applied electric field produces a non-statistical orientation so that the anisotropic properties of the medium are observed. The parallel and perpendicular indices of refraction are related to the applied field $\vec{E}$ by

$$\Delta n = n_{\parallel} - n_{\perp} = KnE^2 \qquad (2\text{-}1)$$

---

*All references are gathered in Section 10.

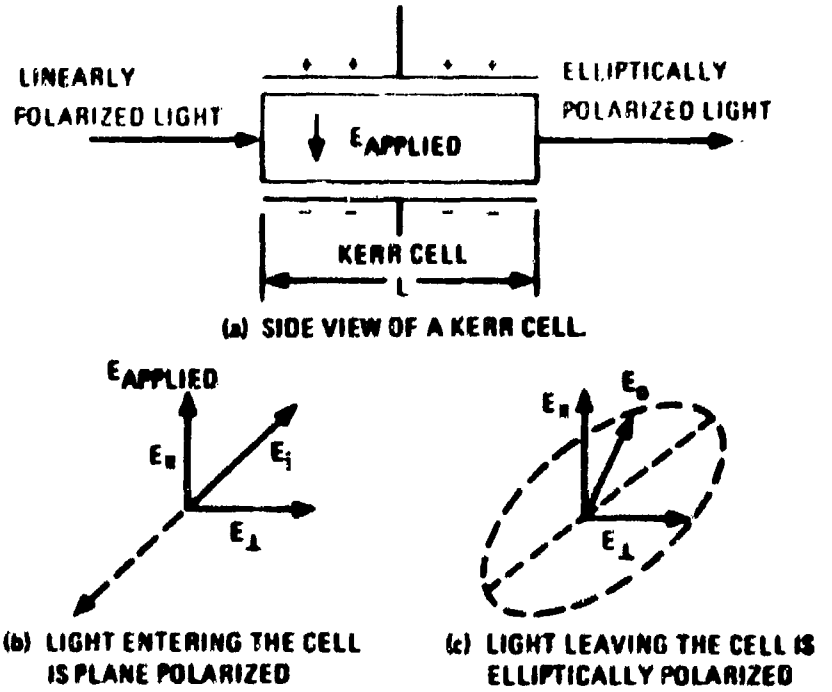

Figure 2-1. Kerr Effect

where n is the mean refractive index, K is a material dependent constant and $n_{\parallel} > n_{\perp}$ represent the parallel and perpendicular components of the refractive indices respectively. Tables of values for the material constant K at optical frequencies are given in Reference 1.

The mean refractive index, n, is related to the material permittivity ϵ and the materials permeability, μ, by the Maxwell relation,

$$n = (\epsilon\mu/\epsilon_o \mu_o)^{1/2} \tag{2-2}$$

where ϵ_o is the permittivity of free space (8.854×10^{-12} coul^2/n-m^2) and μ_o is the permeability of free space. The phase velocity v_p of a light beam passing through the medium with permittivity ϵ becomes

$$v_p = c/n \tag{2-3}$$

where c is the speed of light. Hence, phase velocity is inversely proportional to the square root of the permittivity of the material. From this point ϵ will refer to the relative permittivity, ϵ/ϵ_o.

The optical path length of the Kerr cell shown in Figure 2-1 for the parallel component of the light beam is

$$N_{\parallel} = L n_{\parallel}/\lambda_o \tag{2-4}$$

where $N_{\parallel}$ is the number of wavelengths of light in the cell of length L, $n_{\parallel}$ is the parallel light component index of refraction, and λ_o is the wavelength of light in a vacuum.[2] Similarly, the equation for the perpendicular component,

$$N_{\perp} = L n_{\perp}/\lambda_o \tag{2-5}$$

From equations 2-4 and 2-5, the optical path length difference ϕ expressed in radians, becomes

$$\phi = 2\pi(N_{\parallel} - N_{\perp})$$

$$= 2\pi L \Delta n/\lambda_o \tag{2-6}$$

where $\Delta n = n_{\parallel} - n_{\perp} = K n E^2$

The following analogy can be made for the variable permittivity phase shifter cell that operates in the microwave frequency spectrum. Equation 2-1 remains valid since it is independent of the wavelength of any signal passing through the medium. Equations 2-2 and 2-3 apply to propagation of electromagnetic waves at any frequency. The number of wavelengths N in a phase shifter cell of length L is

$$N = L/\lambda \tag{2-7}$$

where λ is the wavelength of the microwave signal in the medium. In terms of the wavelength of the microwave signal in free space λ_s the wavelength in the medium is reduced by the index of refraction n where

$$\lambda = \lambda_s/n \tag{2-8}$$

Substituting equation 2-8 into 2-7, the number of wavelengths in the phaser cell for the parallel and perpendicular directions in terms of the free space electromagnetic wavelength becomes

$$N_{\parallel} = L n_{\parallel}/\lambda_s \tag{2-9}$$

and

$$N_{\perp} = Ln_{\perp}/\lambda_s \tag{2-10}$$

The microwave phase delay in degrees is

$$\phi = 360^\circ L \Delta n/\lambda_s \tag{2-11}$$

or

$$\phi = 360^\circ LKnE^2/\lambda_s \tag{2-12}$$

The Kerr constant K in equation 2-12 needs to be evaluated for the artificial dielectric material in the microwave frequency region.

In the microwave region, it is preferable to use the dielectric constant rather than the index of refraction in equation 2-12. The dielectric constant can be related to the index of refraction using equation 2-2 and the fact that $\mu = \mu_0$ for the systems under consideration.

Thus, $n^2 = \epsilon$ and we find that $\Delta n = (1/2n)\,\Delta\epsilon = \Delta\epsilon/2\sqrt{\epsilon}$.

The microwave phase delay of equation 2-11 can thus be rewritten in terms of the change in the parallel and perpendicular components of the dielectric constant $\Delta\epsilon$ as

$$\phi = 360^\circ \frac{L}{\lambda_s} \frac{\Delta\epsilon}{2\sqrt{\epsilon}} = 360^\circ \frac{L}{\lambda_s} K\sqrt{\epsilon}\, E^2 \tag{2-13}$$

It is useful to define a specific Kerr constant K_{sp} if the dielectric is constructed by suspending one substance in another. The specific Kerr constant may be defined as

$$K = C_v K_{sp}$$

where C_v is the volume fraction of the suspended component. This relation indicates that at relatively low particle densities the effect of adding more particles to the fluid linearly increases the Kerr constant. The quantity $\Delta\epsilon$ will be analyzed in more detail keeping in mind that equation 2-13 converts the $\Delta\epsilon$ information readily into phase shift information.

2.3 ARTIFICIAL DIELECTRIC

The dielectric material used in the liquid phase shifter cell has conductive particles suspended in a dispersion medium. The mixture is called an artificial dielectric because it is an heterogeneous mixture of microscopic particles rather than an assembly of free atoms or molecules. In general, an artificial dielectric exhibits magnetic dipole polarization as well as electric dipole polarization. Since the dipole polarization varies for different directions in the applied electric field, the artificial dielectric demonstrates anisotropic properties. The combined effect of all the particles in the dielectric under the influence of an external electric field is to produce a net average dipole polarization. The net effect of the particle dipole moments in the medium may be evaluated by either the classical Lorentz theory of real dielectrics or with Maxwell's equations.[3]

If the conducting particles are asymmetric and are free to rotate in the dispersion medium, the orientational polarization can be controlled by an applied electric field, and a variable permittivity liquid dielectric results. The present research effort investigates a microwave artificial liquid dielectric material that consists of an inert solvent and a high density suspension of minute, asymmetric conducting platelets. The variable phase delay properties of the artificial dielectric are attributed to the asymmetry of the individual particles. Under zero electric field, the particles are randomly oriented and are in constant thermal motion. When an electric field is applied to the medium, the surface charges on the individual particles rearrange (polarize) in such a way that they become minute electric dipoles. On the average, the particles experience an aligning torque and will position their long axes with the applied field lines. The permittivity along the field direction varies as a function of the particle alignment. Hence, a microwave signal propagating through the medium with its electric field vector parallel to the bias field vector experiences a phase delay that is a function of the bias field strength.

The electrons in the asymmetrical conducting particles are isolated on each platelet so that the only electron motion possible in the presence of an applied field is a displacement of the positive and negative charges of the particles in opposite directions. Once this charge separation occurs, the particles are polarized and possess an induced dipole moment. These dipoles as a group produce their own field. On a molecular scale, the fields of the individual dipoles are analyzed. On the other hand, a macroscopic analysis considers the average fields produced by a large number of particles (dipoles). The artificial dielectric will be analyzed from the macroscopic point of view. This approach is justified provided that the distance between the dipoles is greater than the dimensions of the dipole so that there are no interactions between dipoles.

2.4 THE KERR EFFECT OF METALLIC SUSPENSIONS

2.4.1 KERR EFFECT MAGNITUDE

O'Konski[4] has considered the theory of electric field induced orientation of metallic suspensions. Until this work no data has been available for the testing of O'Konski's theory, which is now outlined here.

In this treatment it will be assumed that the metallic particles in suspension will be ellipsoids of revolution with two characteristic lengths a and b, with a equal to the symmetry axis. Figure 2-2 shows the two possible configurations which are oblate $a < b$, and prolate $b < a$ spheroids. Oblate spheroids are approximations to disk-like particles and prolate spheroids are approximations for needle-like particles. Let θ be the angle of the symmetry axis, a, with the direction of some externally applied bias field $\ddot{E}$, as shown in Figure 2-3. If C_v is the volume fraction, $C_v = V_2/(V_1 + V_2)$ of the metal particles of volume V_2 suspended in the dispersion medium of volume V_1, and θ is the orientation angle and g_i an optical anistropy factor, then the birefringence Δn can be written as:

$$\Delta n = \frac{C_v}{n} (g_a - g_b) \Phi(\theta) \tag{2-14}$$

where $\Phi(\theta)$ is the induced orientation factor given by

$$\Phi(\theta) = \int_0^{\pi} f(\theta) \left(3 \cos^2 \theta - 1\right) 2\pi \sin(\theta)\, d\theta \tag{2-15}$$

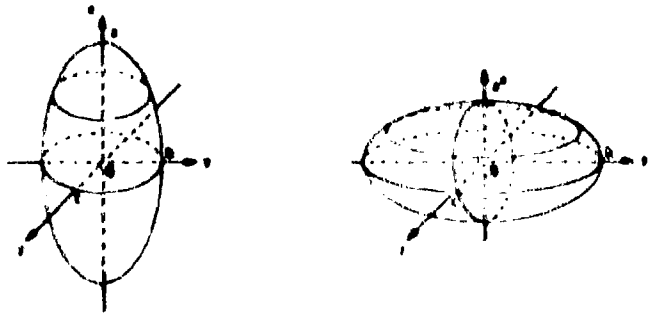

Figure 2-2. Views of Prolate and Oblate Spheroids

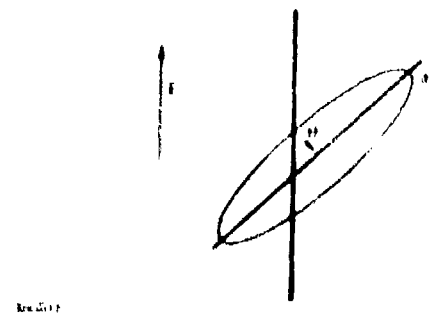

Figure 2-3. Orientation Angles for Ellipsoids in a Bias Field

The function $f(\theta)$ is the probability per unit solid angle of finding the symmetry axis direction with angle θ. Using the Boltzman statistical mechanical method this function depends on the energy of a particle, W.

$$f(\theta) = e^{-W/k_B T} \Big/ \left[\int_0^{\pi} e^{-W/k_B T} \, 2\pi \sin(\theta) \, d\theta \right] \qquad (2\text{-}16)$$

where k_B is the Boltzmann constant and T the absolute temperature in Kelvin.

Maxwell has calculated the anistrops factor $(g_a - g_b)$ for ellipsoids which have three principal moments of refraction along the symmetry axes:

$$g_j = \frac{1}{4\pi} \frac{n_j^2 - n^2}{1 + (n_j^2/n^2 - 1) A_j}, \quad \text{for } j = a, b, \text{ and } c \qquad (2\text{-}17)$$

This theory applies to immersing ellipsoids with depolarization ratio A_j along the axis j of the ellipsoid in a medium of index of refraction n.

The depolarization ratio A_j is calculated using the integral for general ellipsoids where j runs over the axes a, b, and c

$$A_j = \int_0^{\infty} \frac{abc \, ds}{2(j^2 + s) \left[(a^2 + s)(b^2 + s)(c^2 + s)\right]^{1/2}} \qquad (2\text{-}18)$$

Thus the function in equation 2-17 takes account of the two important asymmetry effects for ellipsoids. One is the purely geometrical anisotropy accounted for by the A_j term and the other is the anisotropy due to the different principal moments of induced polarization accounted for by the n_j term.

The total energy W of a particle can be divided into two parts, $W = U + V$, the one part, V, is the energy of the particle not due to its orientation. The other part, U, is that due to the energy of orientation in the external bias field. This energy can be written down by assuming that the field $\vec{E}$ induces a dipole moment on the spheroid with orientation θ. This energy is given by

$$U = -\frac{1}{2}(\alpha_a - \alpha_b) F^2 \cos^2\theta \qquad (2\text{-}19)$$

where α_j is the polarizability along the j-symmetry axis, and F is the field experienced by the particle in the interior of the dielectric. This field for low particle densities is $F = E(\epsilon + 2)/3$. See Böttcher, reference 5.

For metallic ellipsoids suspended in an insulating medium, expressions can be obtained for σ_j and g_j which depend only on the shape and size of the particles. This can be done using the following equation for the excess polarizability along the j^{th} axis,

$$\alpha_j = \frac{v}{4\pi} \frac{\epsilon_j - \epsilon}{\left(\frac{\epsilon_j}{\epsilon} - 1\right) A_j}, \qquad (2\text{-}20)$$

where v represents the volume of the particle, ϵ is the dielectric constant of the medium, and ϵ_j refers to the principal moment dielectric constants of the particle. The Maxwell relation $\epsilon = n^2$ relates the index of refraction to the dielectric constant. For conducting particles in the range of frequencies below the optical region, $\epsilon_j >> \epsilon$. As a result, the difference of the excess polarizabilities $(\alpha_a - \alpha_b)$ can be written[4]

$$\alpha_a - \alpha_b = \frac{v\epsilon}{4\pi}\left(\frac{1}{A_a} - \frac{1}{A_b}\right). \qquad (2\text{-}21)$$

Similarly the anisotropy factor becomes

$$(g_a - g_b) = \frac{\epsilon}{4\pi}\left(\frac{1}{A_a} - \frac{1}{A_b}\right). \qquad (2\text{-}22)$$

Using equation 2-14, the change in dielectric constant is written as

$$\Delta\epsilon = 2 C_v (g_a - g_b) \Phi(0) \tag{2-23}$$

For fields $\vec{E}$, which are small compared to $k_B T$, that is under those circumstances in which the field does not perturb the configurational energy W, the change in dielectric constant can be calculated by

$$\Delta\epsilon = \frac{v\epsilon}{240\pi} \left(\frac{1}{A_a} - \frac{1}{A_b}\right)^2 C_v E^2 \frac{(\epsilon + 2)^2}{9 k_B T} \quad . \tag{2-24}$$

This equation applies in the limit of low C_v when the concentration of particles is small. In this case, a specific Kerr constant can be derived that depends only on the geometrical properties of the particles, or

$$K_{sp} = \frac{v\epsilon}{240\pi k_B T} \frac{(\epsilon + 2)^2}{(9)} Q^2 \tag{2-25}$$

where

$$Q = \left(\frac{1}{A_a} - \frac{1}{A_b}\right) \tag{2-26}$$

Thus the change in dielectric constant is

$$\Delta\epsilon = C_v K_{sp} E^2 \quad . \tag{2-27}$$

Up to this point $\Delta\epsilon$ has been defined as $\epsilon_{\parallel} - \epsilon_{\perp}$ where the subscripts refer to orientations parallel and perpendicular to the applied field. In the phase shifter arrangement, where the electromagnetic field is in a TE_{10} mode, the change of dielectric constant is referred to $\Delta\epsilon' = \epsilon_{\parallel} - \epsilon_{\perp}$.

At this point the value of this theory can be found by displaying the importance of various parameters of the system in obtaining large phase shifts. The parameters of most importance are the loading density or volume fraction of the particles C_v, the volume of the individual particles, v, and the shape ratio, $A = (a/b)$. Let $Q = (1/A_a - 1/A_b)$ be called the shape factor. It turns out that $A_a = 2A_b - 1$ so that Q can be rewritten in terms of A_b only.

$$Q = \frac{3A_b - 1}{A_b(1 - 2A_b)} \qquad (2\text{-}28)$$

Figure 2-4 shows the functional dependence of A_a and A_b on δ, the shape ratio. When a = b, or $\delta = 1$, $A_a = A_b = 1/3$. The regions to the right of this point correspond to needle-like particles while the left region corresponds to disc-like particles. Figure 2-5 shows A_a and A_b over the disc region on an expanded scale. Next, the important function Q is shown (Figure 2-6) calculated from $\delta = 0$ to 2. It can be seen that Q does not strongly depend on δ until the shape ratio is less than 0.2, corresponding to a:b = 1:5. The crucial dependence of K_{sp} on Q^2, seen in equation 2-25, is emphasized by the plot of Q^2 vs δ in Figure 2-7. Hence, the effective shape ratios for phase shifting occur only for values of $\delta < .05$ or a:b = 1:20.

The conclusion from examining the parameter δ, is that the shape ratio is an extremely important function in determining phase shifting characteristics.

Unfortunately, the volume of the particles enters as a linear parameter in equation 2-25 so larger particles are preferred for good phase shifting characteristics. This effect is important since fast response times require small particles while large particle sizes tend to give large phase shifts. To an extent, the factor of v in equation

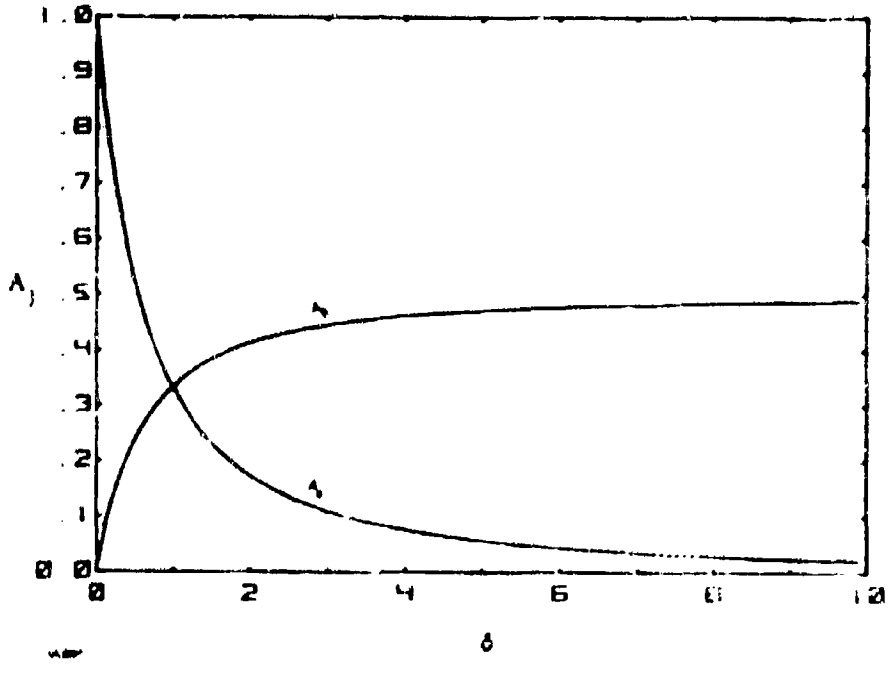

Figure 2-4. Depolarization Ratio Dependence (A) on Shape Ratio (δ)

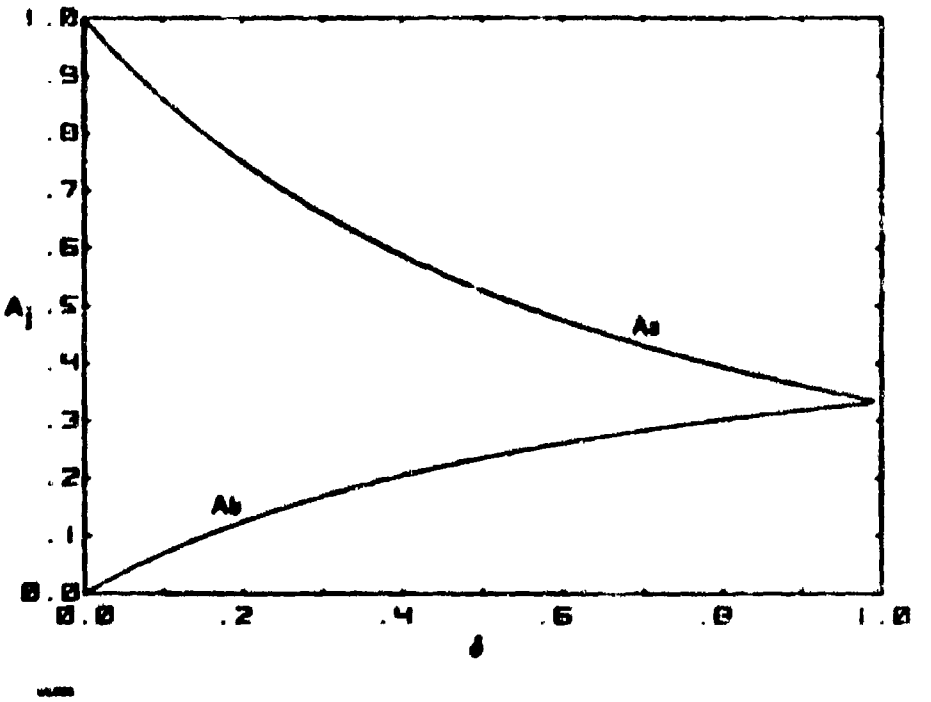

Figure 2-5. Depolarization Ratio Dependence (A) on Shape Ratio (δ) in the Disc-Like Region

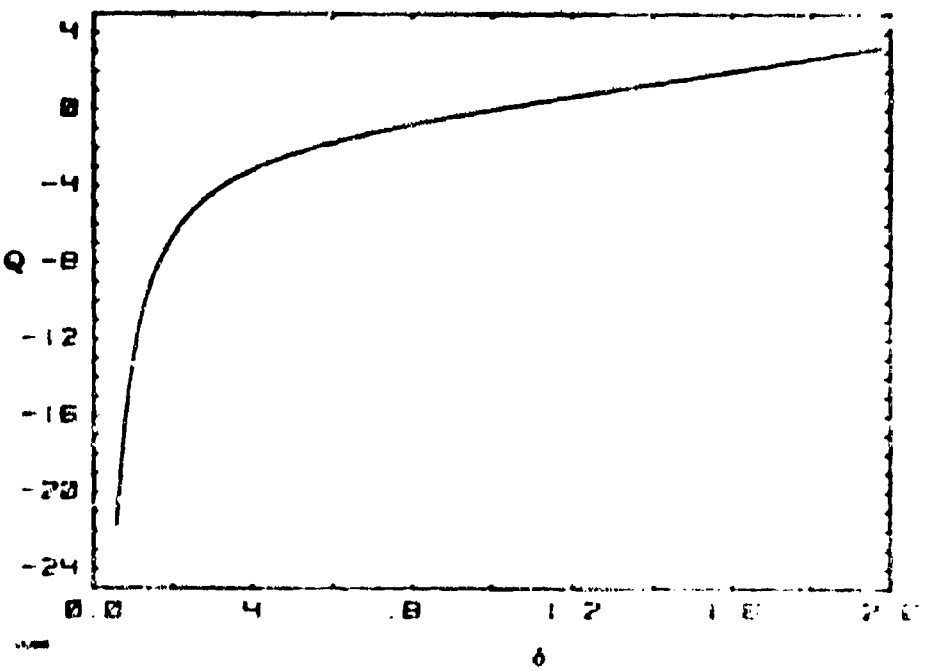

Figure 2-6. Anisotropy Shape Factor (Q) Dependence on Shape Ratio (δ)

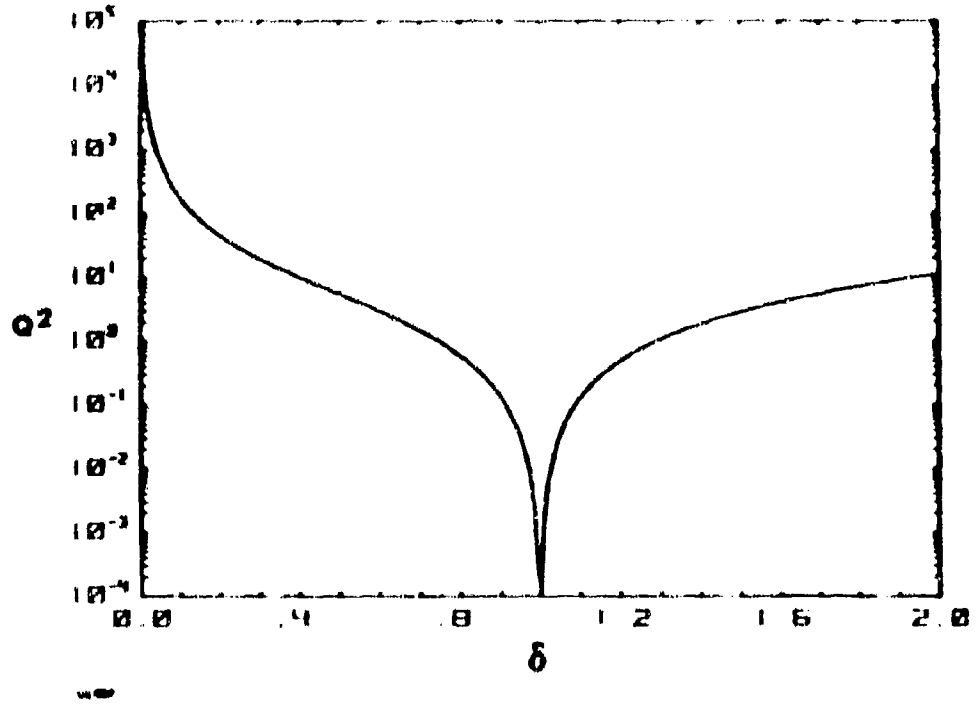

Figure 2-7. Square of Shape Factor (Q) Dependence on Shape Ratio (δ)

2-25 can be offset by increasing the loading density of the particles which considerably mitigates the problem. Due to the polydispersity of particle shapes and sizes, this effect has not yet been evaluated experimentally. At this point the product of vC_v which occurs in the change of dielectric constant expression 2-24 can be assumed adjustable for maximum effect at low loading densities.

Two additional problems which consider the magnitudes of the expected Kerr effect with metal particles include possible saturation and sample polydispersity. Saturation effects are observed when the Kerr effect is no longer proportional to E^2. Polydispersity is caused by a variety of size and shape particles in the medium.

2.4.1.1 HIGH FIELD CASE -- In obtaining equation 2-24 from 2-23, the integrals in the expression for Φ (equation 2-15) were evaluated by assuming that U/kgT was small compared to 1, thus the exponentials were expanded in powers of E^2 using the orientational energy function in equation 2-19. If it is no longer possible to ignore the gross orienting effect of the bias field on the metal particles, these integrals must be evaluated numerically. If a function γ is defined as

$$\gamma = \left[-\frac{(\alpha_a - \alpha_b)}{(2k_B T)} \right] E^2 , \qquad (2\text{-}29)$$

then Φ can be calculated as a function of γ. This function is plotted for values of $\gamma = 0$ to 25 in Figure 2-8. The linear region for $\gamma = 0$ to 5 corresponds to the region of validity of equation 2-27, while for $\gamma > 5$ saturation effects begin to become important. The function γ can be rewritten as

$$\gamma = \frac{v \epsilon Q}{8\pi k_B T} E^2 \qquad (2\text{-}30)$$

Thus, saturation effects become important when the particle size, the shape function (Q), or the ratio $E^2/k_B T$ gets too large. During this contract period consequences of saturation and polydispersity have been observed. However, the effects have not been investigated in depth.

2.4.1.2 POLYDISPERSITY AND THRESHOLD EFFECTS — Because of the systems used in this study, the problems of particle polydispersity are particularly important because the aluminum and magnesium particles used were not the same size and shape. The theory so far presented assumes that the particles are all of the same

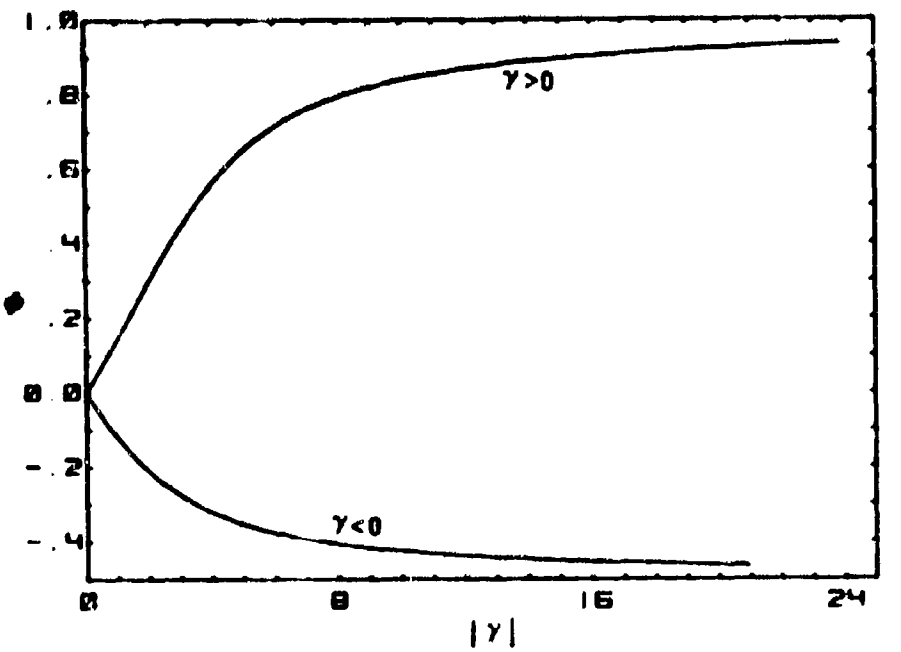

Figure 2-8. Dependence of Orientation Factor (Φ) on Boltzman Factor (γ)

size and shape. The effect of polydispersity can be accounted for by defining an average specific Kerr constant $\bar{K}_{sp}$ by using a shape and size distribution function, $f(\ell, \delta)$. This distribution function gives the probability of finding a particle in the size range ℓ to $\ell + d\ell$ and of shape ratio δ to $\delta + d\delta$. The average specific Kerr constant is defined as:

$$\bar{K}_{sp} = \iint K_{sp}(\ell, \delta)\, f(\ell, \delta)\, d\ell\, d\delta \qquad (2\text{-}31)$$

For relatively sharp distributions of $f(\ell, \delta)$ around some value of ℓ_0, δ_0 equation 2-27 can be used effectively. However, if the distribution δ is not sharp, then the threshold effects become very important. If the particle size and shape distribution is very broad and unsymmetrical then the behavior of K_{sp} at threshold depends very strongly on the applied voltage. Apparently at low field strengths the torque applied by the bias field to the particle must overcome an energy barrier to rotation. Frenkel has examined theories of viscosity which may account for this observation.[6]

Equation 2-24 can be rewritten in terms of the shape function Q as equation 2-32a which upon rearrangement yields equation 2-32b.

$$\Delta\epsilon = \frac{\nu\epsilon}{240\pi}\left(\frac{\epsilon + 2}{3}\right)^2 Q^2 \left(\frac{E^2}{k_B T}\right) C_v \qquad (2\text{-}32a)$$

$$\frac{\Delta\epsilon}{\epsilon}\frac{240\pi}{\left(E^2/k_B T\right)}\left(\frac{3}{\epsilon + 2}\right)^2 = \nu Q^2 C_v \qquad (2\text{-}32b)$$

The function on the left (to be called Z) is useful to indicate the applicability of the theory being used. Figure 2-9 shows a plot of

$$Z = \frac{240\pi}{\left(E^2/k_B T\right)}\left(\frac{3}{\epsilon + 2}\right)^2 \frac{\Delta\epsilon}{\epsilon} \qquad (2\text{-}33)$$

versus C_v for several applied bias voltages using Silberline "AA" aluminum in CCl_4. A line of constant slope $m = \nu Q^2$ should be obtained. This function might be called the effective specific Kerr constant. In fact, several lines of constant slope are obtained indicating less and less slope for higher voltages. If the shape factor Q^2 is assumed to be constant for the different particle sizes, then the conclusion that must be reached is that the average effective volume of the particles must decrease with increase of applied field. This is just the expected result if we assume that applied field strength E_{ap} only affects those particles large enough such that the applied field energy is larger than the barrier to rotation.

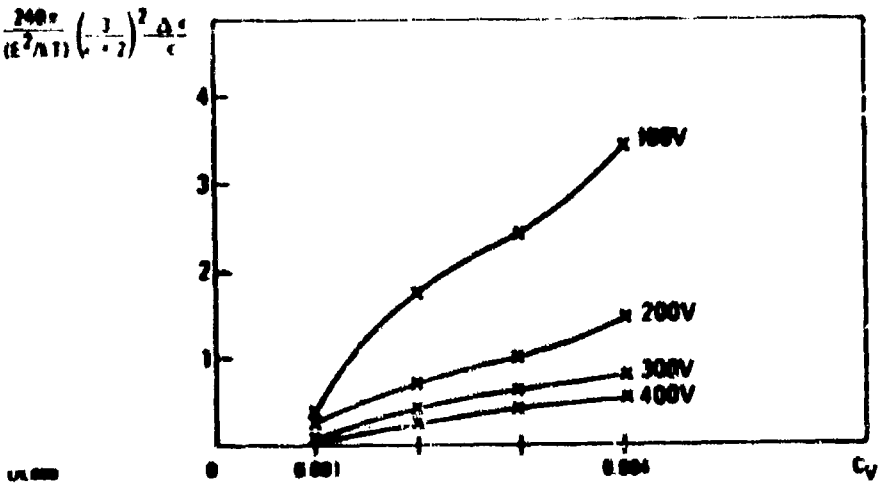

Figure 2-9. Effective Specific Kerr Constant Against Volume Fraction of Second Component

This conclusion shows the tremendous importance in the future for fully investigating the effects of size and shape on the phase shifting ability of fluids. Ultimately, it opens up the possibility of constructing suspension dielectrics with designed particle distributions to achieve fast response time and large stable phase shift.

2.4.1.3 TEMPERATURE AS A PARAMETER — The temperature of the sample affects its phase shift ability by changing $\Delta\epsilon$ in two ways. The first is the obvious functional dependence of K_{sp} in the negative first power of T. By using observed values for metallic suspensions we can obtain the expected temperature coefficient of phase shift as follows:

$$\frac{\partial \Delta\epsilon}{\partial T} = \frac{\partial}{\partial T}(K_{sp})\, C_v E^2 = -\frac{1}{T} K_{sp}\, C_v E^2 = \frac{-1}{T}\,\Delta\epsilon \qquad (2\text{-}34)$$

For a change in dielectric constant of 0.7, which is often observed at 300 °K, $\partial\Delta\epsilon/\partial T = -.002$.

Using equations 2-25 and 2-27 the change in phase shift per degree K can be written

$$\frac{\partial \phi}{\partial T} = -\frac{1}{T}\,\phi \qquad (2\text{-}35)$$

for 360° phase shift at 300° K this corresponds to a temperature coefficient of $-1.2°/°K$ which is in good agreement with that observed by Buscher (1972).[7]

2.4.2 RESPONSE TIME AND RELAXATION PHENOMENA

The theory of the response of metal suspension artificial dielectrics to a polarizing field has been considered by numerous authors and reviewed extensively by O'Konski[4] (1972). As noted in 2.4.1, these theories primarily consider monodisperse suspensions, that is, suspensions of one size and shape, whereas the systems being used in this study are polydisperse. Thus we feel that at present only the qualitative results from the theory can be used as a guide to the properties of our systems.

A particle in the medium experiences several torques over a period of time. There is an orienting torque due to the bias electric field and Brownian motion fluctuations which cause random uncorrelated, instantaneous changes in the orientation. Finally the medium produces friction when the particle rotates in it. The differential equation of the orientation function $f(\theta)$ as a function of time can then be written[8, 9]:

$$\frac{1}{\mathfrak{C}} \frac{\partial f(\theta, t)}{\partial t} = \frac{\partial}{\sin \theta} \frac{\partial}{\partial \theta} \left[\sin \theta \left(\frac{\partial f(\theta, t)}{\partial \theta} - \frac{M}{kT} f(\theta, t) \right) \right] \qquad (2\text{-}36)$$

where θ is the angle of the symmetry axis with the applied field and M is the magnitude of the torque of the applied field. The frictional losses of rotation are contained in the rotational diffusion constant $\mathfrak{C}$. This equation assumes that inertial terms are not present since the energy of rotation is small compared to the Brownian motion impact energies. This equation thus cannot predict any overshoot of the phase shift.

For a given amount of dielectric constant change $\Delta\epsilon'_0$ at some field strength, the solution to 2-36 gives this simple exponential law:

$$\frac{\Delta\epsilon'(t)}{\Delta\epsilon'(0)} = e^{-t/\tau} \qquad (2\text{-}37)$$

$$\tau = \frac{1}{6} \Theta$$

where the relaxation time is τ. (Benoit 1951; O'Konski and Zimm 1950).

We have not extended this theory to polydisperse samples at this time for two reasons. First, the data indicates that only one characteristic relaxation time is present so that empirical values for τ can be obtained. Second, with no knowledge of the functionality of $f(\ell, \delta)$ more sophisticated theories are not useful.

Figure 2-10 shows the process of changing permittivity for a field switched on and then off. In the simplified theory used here the equation for buildup is:

$$\frac{\Delta\epsilon'(t)}{\Delta\epsilon'(\infty)} = 1 - e^{-t/\tau} , \qquad (2\text{-}39)$$

where

$$\tau = \frac{1}{6\Theta}$$

The assumption of this model, therefore, is that the buildup time is approximately equal to the relaxation time. Although evidence has been found that τ_r and τ_f, the characteristic rise and fall times, are different, we feel that the data is not of sufficient quality to justify too much dependence on their values. In the simple theory $\tau_r = \tau_f$. A consideration of the functional dependencies of τ on various parameters will give an idea of the possibilities for improvement of τ_r. The rotational diffusion constant depends on the viscosity, η, the characteristic particle radius, ℓ, the temperature, T, and a shape factor, Q', similar to the previously defined Q in the following way:

$$\Theta = \frac{\ell^3 Q'}{k_B T}\eta . \qquad (2\text{-}40)$$

The characteristic particle radius is equal to the length of the longest axis. Since $\tau_r = 1/6\Theta$ the improvement of response time is most obviously seen to arise from reduction of the particle size, ℓ. The experimentally observed τ_r for particles of size 5-10μ are on the order of 1-3 sec, so that a reduction of particle size by a factor of 100 to .05-0.1μ should give τ_r of 1-3μsec. As mentioned in 2.4.1 (equation 2-24), there is a tradeoff of total response magnitude with response time. We feel that study

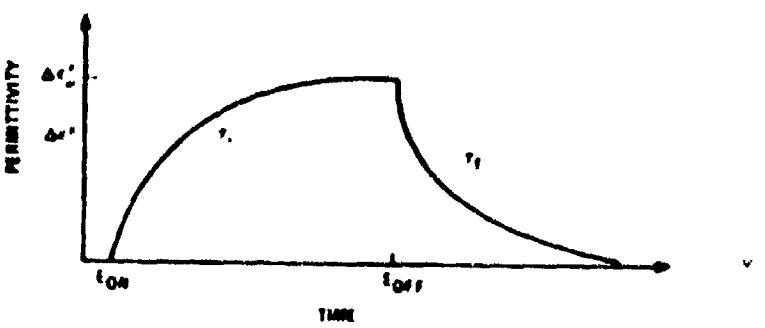

Figure 2-10. Switched-on and Switched-off Behavior of Permittivity Difference ($\Delta\epsilon'$) in the Low-Field Case

along these lines is certainly indicated. The other variables in equation 2-40 enter only in a linear fashion so that only moderate improvements can be expected in τ_r. In particular, the composition of the dielectric as a CCl_4 or CCl_4-CBr_4 suspension limits the range of η variation while the temperature range of 10-50°C is not large enough to substantially change E. The shape factor Q', in general, increases with the asymmetry of the particle, again a result that contends against large changes in $\Delta\epsilon'$. Using the following approximate values for the parameters in equation 2-40 we have calculated a response time of 6 sec, as characteristic of the aluminum particle system. We took T = 300°K, $\ell = 10\mu$, $\eta = 10$ millipoise and Q' = 2.2. The value of $\tau_r = 6$ sec corresponds quite well to the observed values of 1-5 sec for low applied bias fields of 200 volts/cm at 4 kHz.

Figure 2-11 shows a logarithmic plot of the parameter τ_r versus particle size ℓ in microns using the low field case equations 2-39 and 2-40. The three lines arise from use of three values of the shape factor Q' = 0.22, 2.2, and 22.0 corresponding to a shape ratio distribution of a:b from 1:2 to 1:20. The shaded region shows the region of relaxation times and size distributions which have been studied so far. By reducing the size of the particles to ~.01μ, microsecond response times should be realized.

For monodispersive cases O'Konski[4] has considered high field response times and it should be noted that at high field strengths, τ_r should be much smaller than τ_f. We intend in the future to use shaped pulses in driving voltages for given orientations.

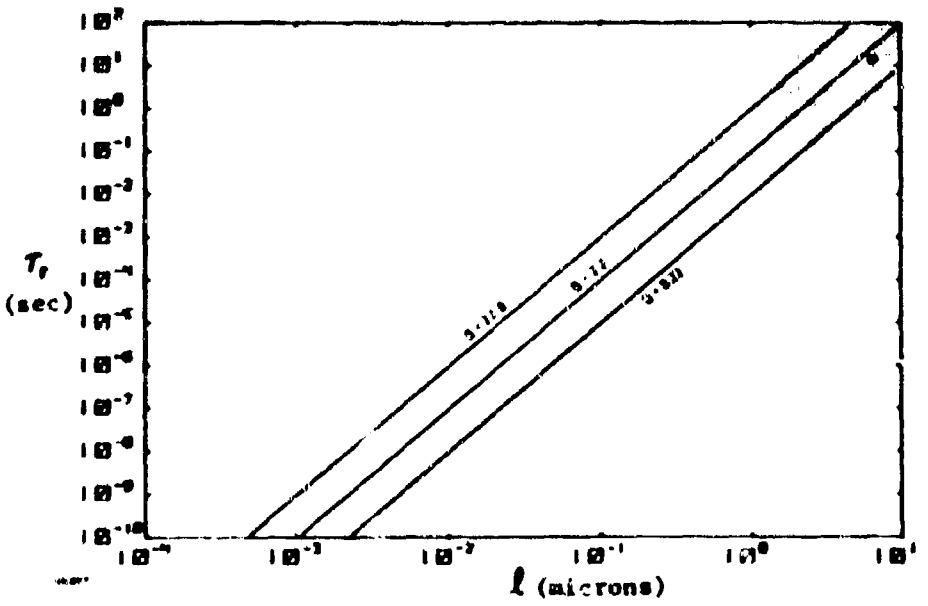

Figure 2-11. Logarithmic Plot of Response Time (τ_r) vs. Particle Size (ℓ) for Different Values of Shape Factor (Q')

Empirically high field strength saturation begins to show above 400 volts/cm at 4 kHz.

Because of breakdown problems in the aluminum system this method was not pursued, but with the more stable magnesium system this work can be reinitiated. Buscher[7] (1972) found, while working with a $h\nu$ band phaser, that giant pulses on the order of 20000 V/cm produced response times on the order of 10 μsec. We feel that additional work in this area is justified.

Thus two methods are available for improvement of relaxation times, high field pulses and particle size reduction.

3. ELECTRODE DESIGN

3.1 DESIGN GOALS

The initial attempt at producing an S-band phase shifter consisted of simply scaling down the existing K_u band version. The first S-band version consisted of a single electrode, approximately 58 cm long, placed in a WR-284 waveguide, with teflon impedance matching wedges mounted on the ends as shown in Figure 3-1. The performance characteristics of this initial test cell design is shown in Figure 3-2. This design was to be the starting point for improvement in electrode design and modification of the S-band phase shifter. To prove the practicality of an experimental model, it was felt that the critical goals in the area of electrode design that should be met were:

- Insertion loss < 1 dB ± .2 dB
- VSWR < 1.2:1
- Control Voltage < 1000 volts rms

3.2 DESIGN REDUCTION OF CONTROL VOLTAGE

Early in the study it became evident that one of the primary goals for realizing a practical phase shifter would be reduction of the applied bias required for operation. The reasons for lower control voltages are self-evident:

1. Reduced electrical insulation needed to prevent breakdown to and within the phase shift cell
2. Reduces need for large, heavy high voltage power supplies required to shift phase

There are a number of viable approaches which can be sought, all of which can be most easily extracted from the Kerr equation

$$\phi = \frac{360^\circ K L}{\lambda_0} nE^2 \qquad (3\text{-}1)$$

The first and most obvious approach is to lengthen the test cell, but there are a number of disadvantages. To decrease the control voltage by a factor of two, the phase shift cell would have to be lengthened by a factor of four resulting in a cell almost nine feet long. Aside from the manifest problems of physically handling this cell and the difficulty of retrofitting it into an existing system, the increased losses due to liquid dielectric (even just CCl_4) would make this approach prohibitive.

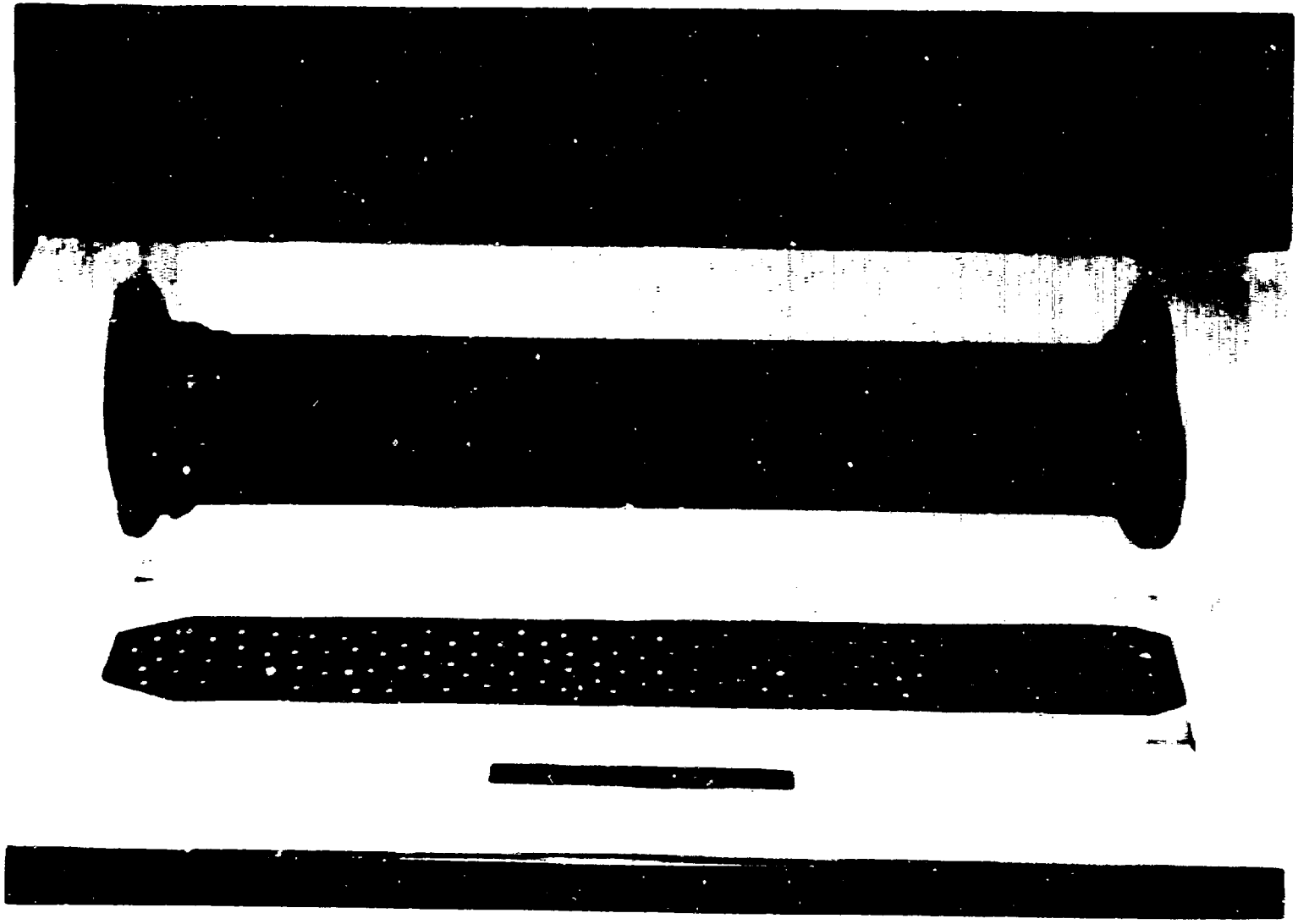

Figure 3-1. S-band Phase Shifter Fabricated Using K_u Band Version

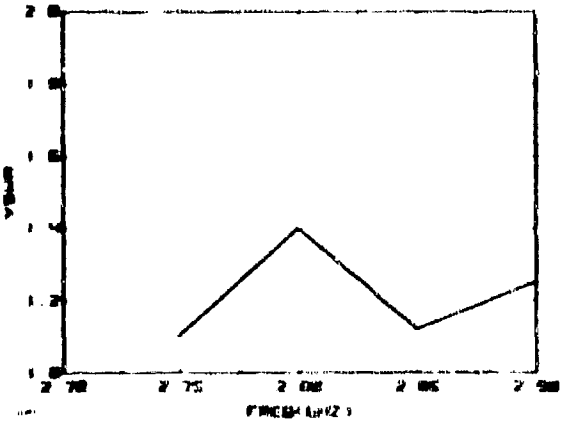

(A) Insertion Loss vs. Frequency

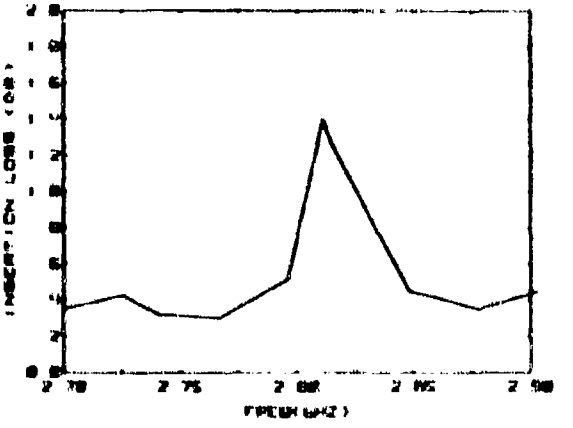

(B) VSWR vs. Frequency

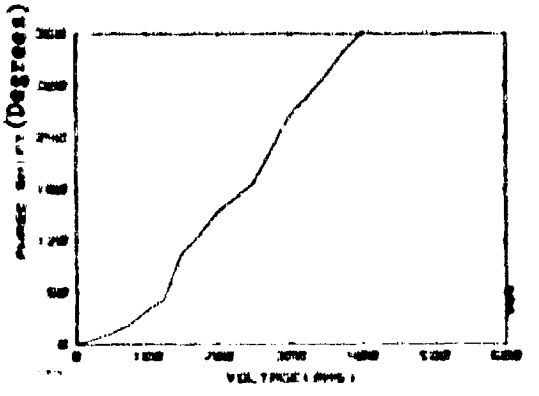

(C) Phase Shift as a Function of Applied Voltage

Figure 3-2. Initial S-Band Phase Shifter Performance

The second approach — successfully employed as part of the material studies — would be to increase the Kerr constant K and thereby obtain improved performance. This has been pursued by varying the number density in the most important of suspension systems, by testing different manufacturer's batches of suspension fluid powder and through new materials research. These results are discussed in a later section, but it is apparent that gains in this area are limited, as in the case of increasing the electrode length, by the $\sqrt{K}$.

The third approach has been in the area of increasing the electric field strength. By referring to the Kerr equation, it is easily seen that by doubling the electric field strength a factor of four increase in the phase shift is realized in the low E field region. The electric field E is related to the applied bias voltage V and the separation of the electrodes d by the relationship

$$E = \frac{V}{d} \tag{3-2}$$

The electric field can be increased in either of two ways. First, the control voltage may be increased (this is not desired); second, decrease the electrode separation. By decreasing the electrode separation by a factor of only two, the control voltage was cut in half. The design chosen (Figure 3-3) was a 3-electrode or periscope configuration that reduces the control voltage to one-third the original value. This configuration reduced the length from 58 to 11 cm. An important comparison is the phase shift per unit length of waveguide cell shown in Figure 3-4.

3.3 DESIGN REDUCTION OF INSERTION LOSS AND VSWR

After extensive testing with the single electrode phase shift cell, it was found that the insertion loss peaks, shown in Figure 3-5, that were being observed in pure carbon tetrachloride and the Al-CCl_4 liquid dielectric were higher-order evanescent modes. Further testing of the single electrode configuration in air verified this supposition with measurements that indicated that the modes were being initiated at the discontinuity of the electrode within the cell. The curves shown in Figure 3-6 were obtained by drilling three holes across the width of the guide to measure the existence of a TE_{20} mode ahead of the electrode, of the electrode discontinuity, and on the electrode.

An obstacle, or discontinuity, will generate higher order modes even when the dimensions of the waveguide are too small for their transmission. In the vicinity of discontinuities rather complicated field distributions prevail, but these may be resolved by Hygens construction methods which indicate the generation of certain higher order modes. However, if the dimensions are such that only the dominant mode can be supported, such waves may not be propagated over any appreciable distances. The load into which these higher order sources look, being a guide operated beyond cutoff, may be regarded as a large negative susceptance. It is not, however, a pure susceptance,

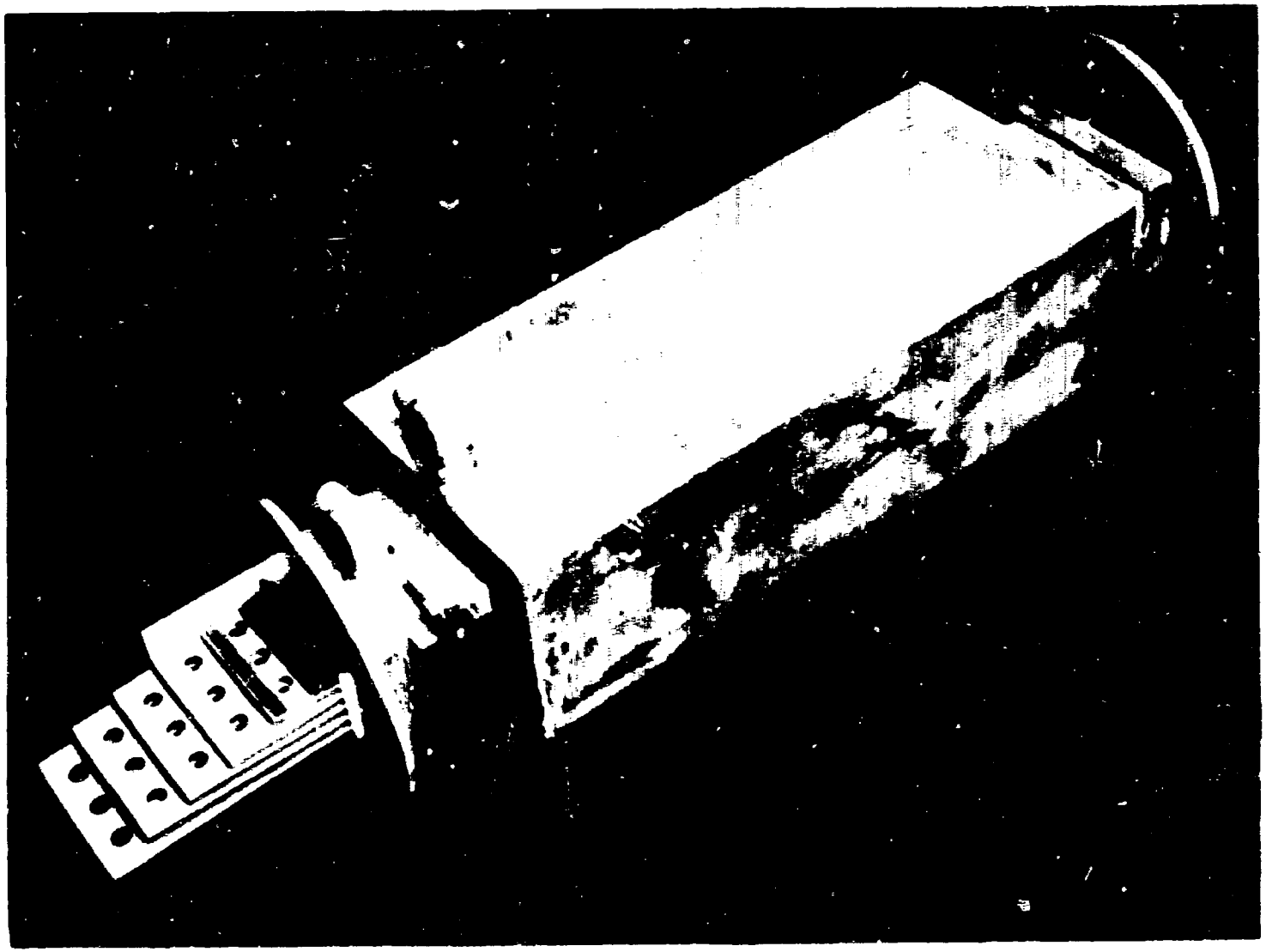

Figure 3-3. Phase Shifter With Pentaplate Electrode Configuration

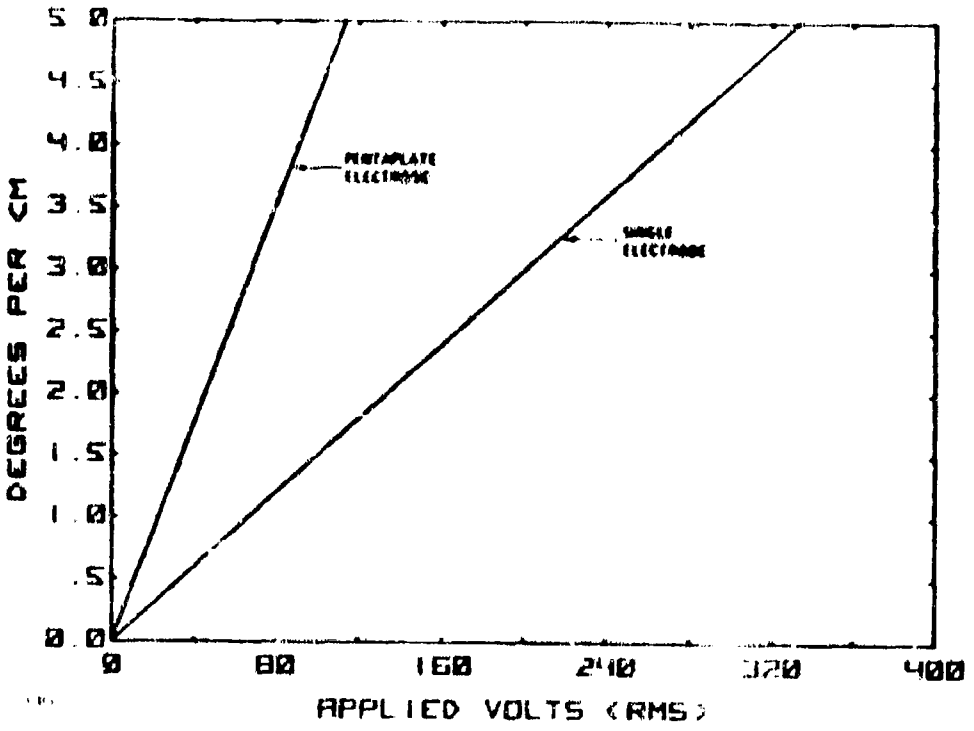

Figure 3-4. Comparison of Phase Shift Obtained for Single and Pentaplate Configurations

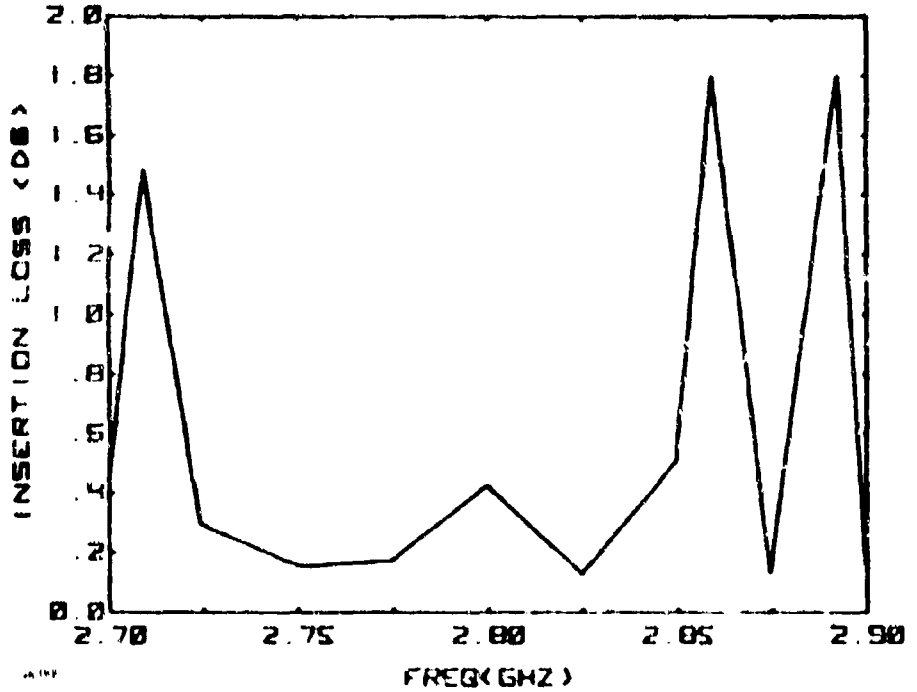

Figure 3-5. Insertion Loss Peaks Caused by Generation of Higher Order Modes

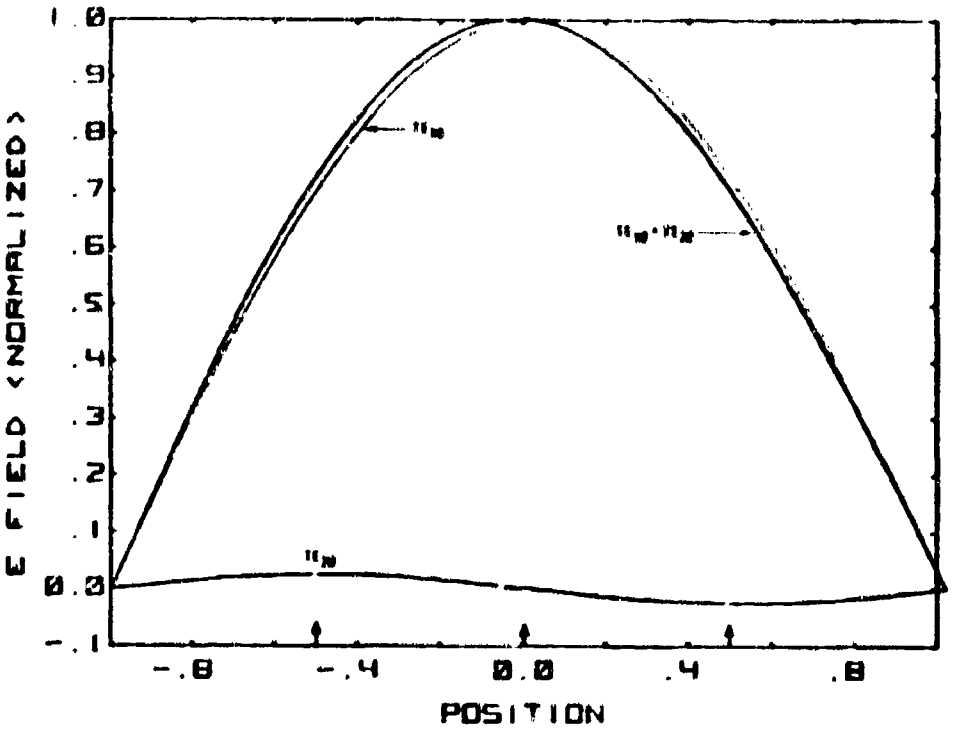

Figure 3-6. Computer Derived Mode Distribution Using Measured Amplitude Distribution Across Waveguide Width

and is not entirely free from loss, for substantial wall currents will exist incidental to the multiple reflection of the higher order waves. Thus, the presence of obstacles leads to dissipation of power. Thus it was felt that a different approach to the understanding and analysis of waveguide discontinuities had to be taken.*

Consider a line terminated in its characteristic impedance and that the discontinuities in the waveguide are lossless, that is $\tilde{Y} = i\tilde{B}$. Then the reflection coefficient r is

$$r = \frac{Y_1}{2M_1 + Y_1} \tag{3-3}$$

where Y_1 is the admittance and M_1 is the characteristic admittance. Normalizing, one obtains

$$r = \frac{\tilde{Y}}{2 + \tilde{Y}} \tag{3-4}$$

*Based primarily on Southworth, Ref. 10.

The reflection coefficient can be related to the VSWR ϕ_v by

$$\phi_v = \frac{1 + |r|}{1 - |r|} = \left[\frac{\sqrt{4 + \tilde{B}^2} + \tilde{B}}{\sqrt{4 + \tilde{B}^2} - \tilde{B}} \right] \tag{3-5}$$

Now, the susceptance, $i\tilde{B}$, is terminated in its characteristic admittance $\tilde{Z}$ where $|\tilde{Z}|$ is defined as

$$|\tilde{Z}| = \frac{1}{\sqrt{1 + |\tilde{B}|^2}} \tag{3-6}$$

and ξ, the angle of the reflection coefficient, is given by

$$\xi = \tan^{-1} \frac{2}{|\tilde{B}|} \tag{3-7}$$

The distance to a nearby voltage minimum is

$$|\tilde{B}|\, d - \frac{\xi}{2} = (2n + 1)\frac{\pi}{2} \tag{3-8}$$

Combining the above, one gets

$$|\tilde{B}| = 2 \tan \left((2n + 1)\frac{\pi}{2} - \frac{4 \pi d}{\lambda_g} \right) \tag{3-9}$$

It should be noted that this development does not take into account the fringing at the discontinuity. For the capacitive case, $\tilde{B} > 0$, the distance to the first voltage minimum is

$$d = \frac{\lambda_g}{4\pi} \left(\frac{\pi}{2} - \tan^{-1} \left(\frac{\tilde{B}}{2} \right) \right) \tag{3-10}$$

This expression identifies where a second discontinuity should be located to correct the mismatch incurred by the first. Since $\tilde{B} > 0$, a discontinuity should be located at a distance

$$\ell = \frac{\lambda_g}{2\pi} \tan^{-1} \left(\frac{2}{\tilde{B}} \right) \tag{3-11}$$

on the generator side of the minimum. If $|\tilde{B}|$ is small, then $2/\tilde{B} \rightarrow \infty$, and

$$\tan^{-1}\left(\frac{2}{B}\right) = \frac{\pi}{2}$$

which gives the spacing between discontinuities

$$\ell = \frac{\lambda_g}{4} \tag{3-12}$$

With this fact, coupled with the pentaplate electrode design, it was decided to space the electrodes, designed around a center frequency of 2.8 GHz, with the electrodes themselves one half the spacing between discontinuities, i.e., $\lambda_g/8$. Tests performed on these electrodes in air and in CCl_4 did not show the characteristic insertion loss peaks previously observed nor were any higher order harmonics ever measured.

The results and comparison of the five plate electrode to the single plate electrode for insertion loss and VSWR as a function of frequency are discussed in Section 7. However, the worst-case insertion loss was less than .5 dB and the worst case VSWR is 1.14:1 for the band 2.7-2.9 GHz, for CCl_4 without Al.

Since the VSWR can be related to $|\tilde{B}|$, then

$$|\tilde{B}| = \frac{\phi_v - 1}{\phi_v^2} \tag{3-13}$$

which corresponds to a $|\tilde{B}|$ of ~ .1077 which deviates less than 3.5% from the ideal case.

3.4 INSERTION LOSS VS. PHASE SHIFT

To obtain a 360° phase shift in the five electrode cell, the permittivity of the liquid must change by an amount sufficient to increase the number of guide wavelengths by one. The waveguide wavelength, λ_g, is a function of permittivity and varies as

$$\lambda_g = \frac{\lambda_o}{\sqrt{\epsilon(E) - (\lambda_o/2a)^2}} \tag{3-14}$$

where $\epsilon(E)$ is the permittivity as a function of the applied field. In the new cell configuration, it is found that a 360° phase shift can be accomplished by a change in

permittivity of ~ .5 (assuming an initial ϵ of ≈ 2.5). However, this can lead to difficulty in meeting the matching condition from last section, namely

$$\ell = \frac{\lambda_g}{4} \tag{3-15}$$

which is also dependent on λg. It is evident that any change in ϵ causes an increase in the mismatch between the spaced sections of each of the electrodes. In this case, a change of .5 leads to a change of ≈ 12% in λg. If the overall length of the phase shift cell is allowed to decrease, the necessary change in ϵ, and, thus, the mismatch (insertion loss) is increased as the phase is shifted.

It is felt that this problem can be limited to about .2-.3 dB by not allowing the cell length to decrease below its present length of 44 cm which limits the necessary permittivity change to ~.5. Also, the electrode design can be modified such that the matching condition (equation 15) is met when the phase is shifted by 180°. Therefore, as bias voltage is applied and the permittivity is changed, the mismatch decreases until λ_g meets the matching condition. As further bias is applied, the mismatch increases until the phase is shifted 360° and the insertion loss is where it was initially as shown in Figure 3-7.

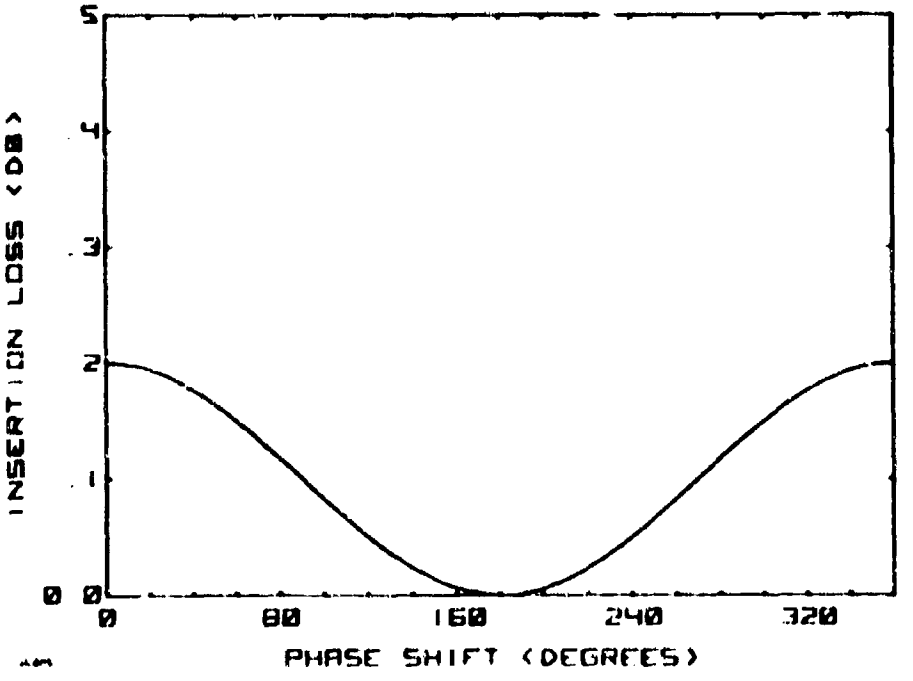

Figure 3-7. Insertion Loss Change as a Function of Mismatch Caused by Changing Permittivity

There is one other source of insertion loss as a function of phase shift — the impedance matching wedges. As the permittivity of the dielectric is increased, an additional mismatch between the impedance matching wedges and the dielectric occurs. This loss is directly related to the change in permittivity. Therefore, as the phase is increased the mismatch and resultant losses can be expressed as

$$\text{Insertion loss} = 20 \log \left(\frac{2\sqrt{\epsilon_1}}{\sqrt{\epsilon_1} + \sqrt{\epsilon_2}} \right) \qquad (3\text{-}16)$$

where ϵ_1, ϵ_2 are the permittivities of the two boundaries; see Figure 3-8. Presently, the material used in the wedges is teflon with $\epsilon_1 = 2.10$. Therefore, as the phase is shifted the increased permittivity results in increased insertion loss. With the present liquid, as the permittivity varies from 2.5 to 3.0, the loss increases from ~0.4 dB to ~0.8 dB. This can be minimized, however, by choosing an impedance wedge with a dielectric constant of approximately 2.75, or choosing a liquid dielectric whose permittivity can be varied between, say, 1.8 and 2.4, matched at 2.1.

3.5 ELECTRODE FABRICATION

With the design change of the electrode configuration it became necessary to change the method of electrode fabrication. In the single electrode phase shifter, the electrodes were fabricated from brass (.010 in.) or aluminum (.030 in.) sheet. These were machined to the proper size and holes randomly drilled in them with the intent of flow enhancement. A lead wire was then attached to the electrode and a teflon coating of ~ 10 mil applied. It was originally feared that insertion loss peaks that were observed were due to electrode alignment in the waveguide, but extensive testing to this point did not bear out this hypothesis. The holes drilled in the electrode did show effects on insertion loss, as discussed in Section 7.

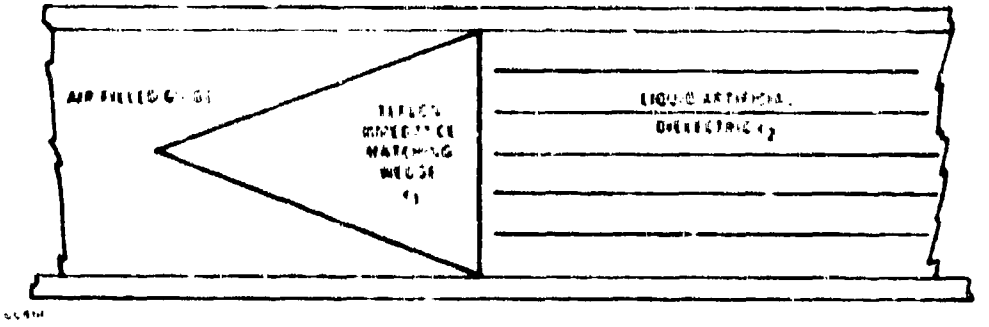

Figure 3-4. Boundary Region Between Phase Shift Cell and Air-Filled Waveguide

With the advent of the five-plate, spaced electrode configuration, it became very obvious that a new means of electrode fabrication was necessary to hold the electrodes accurately in place. A new material, copper clad fiberglass, was employed. The electrode material was a layer of 1.5 mil copper on a ~31 mil fiberglass or mylar backboard. A tape mask, blown up 2 to 1, is laid out and reduced on film and to etch the copper-clad material. Only one film mask is needed and can be used almost indefinitely throughout production. With this method, identical electrodes were produced at an extremely low cost even though they were made in a one-of-a-kind fashion. Both the single and pentaplate electrodes were supported by thin teflon plates (~1/8 in. thickness) with narrow grooves machined in them.

4. PUMPING SYSTEM

4.1 GENERAL DESIGN

The design goals of the S-band phase shifter originally included fabrication of a liquid circulating system with an adequate capacity for keeping the metal particles from settling and for temperature control of the liquid environment. The major problem of the pumping system lies in scaling from K_u-band to S-band.

Since a successful pumping system existed at K_u-band it was felt that scaling to S-band would bring results. But problems became evident almost immediately. The cross-section increases by a factor of 11, but the volume increases by a factor of 600 to 900 depending on which size S-band system was in use. Thus, to turn the liquid over at the same rate as in K_u band, a pump with this increased volume capacity was necessary.

The original flow rate attempted was at a scaling of approximately 6 to 1. The results reflected the amount of thought applied to the problem at the time. Even as more effort was expended on this particular problem it became evident that the flow was limited by the design of the system in operation at K_u-band, Figure 4-1. The major areas of loss seemed to lay in the pressure drop of the debubbling reservoir, the 1/4 in. teflon lines used and the input and output ports of the phase shift cell. The capacity of the pump was also far below what scaling would imply. However, the

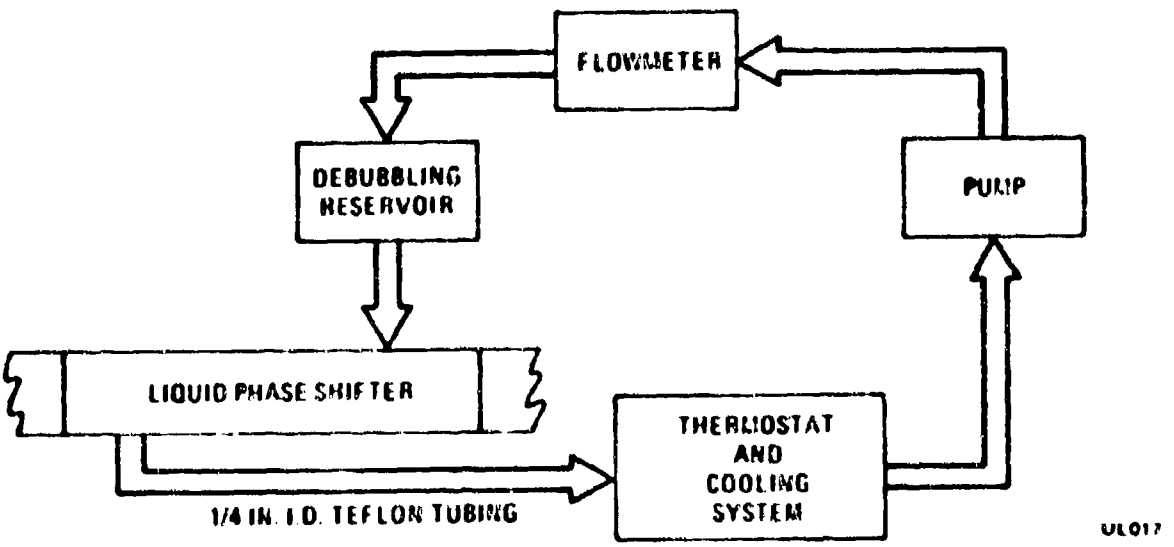

Figure 4-1. Flow System Schematic for K_u-Band Cell

investigations of the effects of flow on permittivity change suggest clearly that increasing the flow was not the answer to the problem of settling. Instead an increased effort to find a new more stable liquid was more promising than any conceivable pumping scheme. This conclusion was forcefully demonstrated by the tests which showed that in some instances pumping decreased the attainable phase shift by more than 75%.

4.2 PARTICLE SETTLING AND FLOW BIREFRINGENCE (MAXWELL EFFECT)

The primary reason for using a pumping system to circulate the liquid dielectric is to prevent the metallic particles in the dispersion medium from settling. However, as will be shown here, the pumping system does not really enhance the stability of the liquid if the flow within the phase shift cell is laminar. Eskinazi[11] has shown that when an incompressible fluid in a state of laminar flow between two stationary solid plates reaches a fully developed state it has a parabolic velocity profile between the plates as shown in Figure 4-2. The flow between plates is described by the Navier-Stokes differential equation; however, the only terms that are not zero are

$$\frac{1}{\rho}\frac{\partial p}{\partial x} = \nu \frac{\partial^2 u}{\partial y^2} \qquad (4\text{-}1)$$

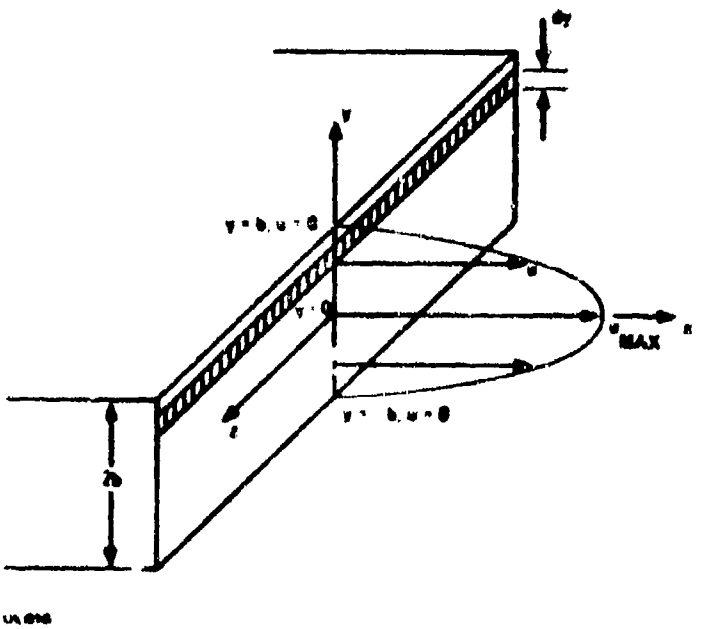

Figure 4-2. Velocity Profile of Liquid Flow Between Two Parallel Plates

p = Hydro-static pressure

ρ = Fluid density

ν = Kinematic viscosity

u = Fluid velocity

Solution of this equation yields the following expression for the fluid velocity:

$$u(y) = u_{MAX}\left[1 - \left(\frac{y}{b}\right)^2\right] \qquad (4\text{-}2)$$

The important thing to note is that the velocity is zero at the walls. Actually one would like the fluid movement at the walls to be largest to prevent the particles from settling and coating. Such is not the case. Thus, if pumping is to prevent settling, then a strongly turbulent velocity profile is required. Comparison[12] of the velocity profiles for laminar and turbulent flow of equal mass flow rates shows that the velocity gradient for turbulent flow is much greater near the walls. Because the velocity of turbulent flow is much more uniform between plates it can also be argued that it would even further reduce the phase shift as compared to that which is obtained for laminar flow or the case without any pumping.

The most adverse effect incurred by the use of a pumping system for suspending particles is that of flow birefringence.[13] A viscous liquid consisting of asymmetric particles that flow in such a way that there is a shearing velocity gradient produce a change in permittivity because of partial particle alignment in the force field of liquid flow. The particles tend to align along the lines of flow and hence reduce the obtainable phase shift. Therefore, a pumping system is not desired, because it:

1) Reduces phase shift obtainable
2) Does not enhance liquid stability
3) Complicates phase shifter design

It turns out that several other approaches lend themselves to prevent particle settling. Among these are:

- Density matching of the dispersing medium to the particles (as discussed in Section 6)
- Utilization of submicron size particles, because Brownian motion keeps these particles in suspension (as discussed in Section 6)
- Development of one-component systems, in which the molecules of the liquid themselves are polar

4.3 TEMPERATURE CONTROL

Among the many reasons quoted, when the development of the phase shifter began, for the use of a pumping system was based on insertion loss data obtained at K_u-band of around 2-3 dB. After further study of the S-band unit and changing to better liquid dielectric materials, the insertion loss was reduced to less than 0.5 dB and thus a pumping system would only be useful for high-power operation. Assuming an average power level of 5 kW and an insertion loss of 0.5 dB, then about 10 % of the power (or 500 watts) are dissipated in the phase shifter and some form of heat removal may be necessary.

Several solutions exist for heat removal from the phase shifter. The first is to attach a set of radiating fins to the phase shifter as shown in Figure 4-3 and as commonly used on high power loads. A second approach for heat removal is a water jacket around the phase shifter cell, with an external heat exchanger attached to the flow lines. The experimental model of the phase shifter cell shown in the Frontispiece has such a water jacket.

Further study may indeed show that no active arrangement for heat removal is necessary; however, a prerequisite for such action is a more thorough understanding of the properties of the liquid at higher temperatures.

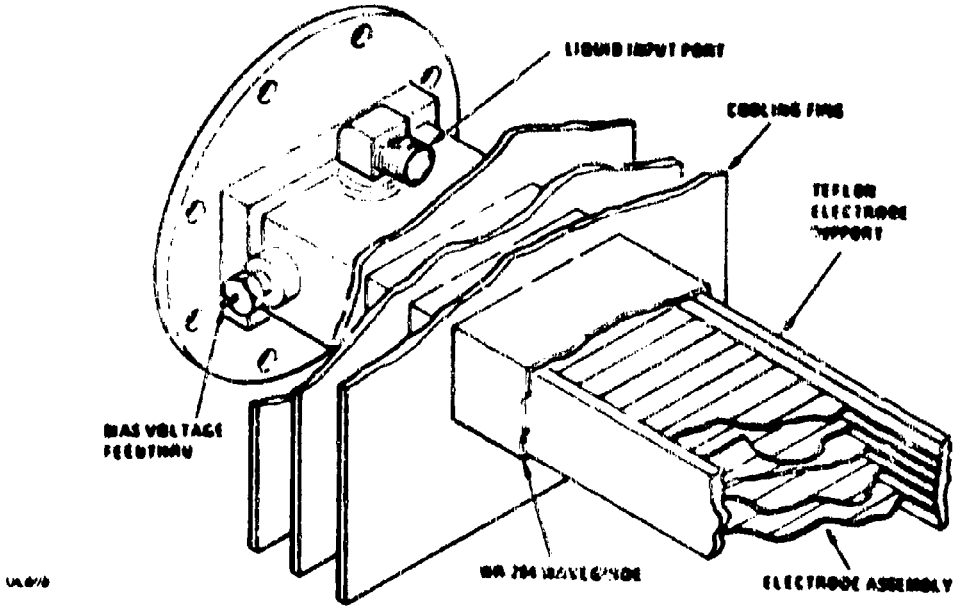

Figure 4-3. Phase Shifter Cell with Cooling Fins

5. MATERIALS AND MATERIAL PROPERTIES

As noted in Section 2, the artificial dielectrics needed for good phase shifting ability must be composed of components with several desirable properties. The search for one-component systems entails the discovery of materials which imitate the artificial dielectric behavior on a microscopic or molecular scale, and, in general, one-component systems must satisfy similar requirements. In addition, the projected use of these materials in devices requires that the liquid dielectrics have certain desirable mechanical and chemical stability properties. Thus, the materials point of view, as expressed in this chapter, is particularly important for understanding the possibilities of liquid phasers and the necessary work to be done in the future.

First the mechanical and chemical properties which are required independent of phase shifting ability will be examined and then the properties applicable specifically to the action of the material in a phaser will be examined. These first discussions will be general in nature. The sections following will cover specific systems studied in this contract in a comprehensive way, system by system.

5.1 GENERAL CONSIDERATIONS OF MECHANICAL AND CHEMICAL STABILITY

The materials used ought to have such obvious properties as being non-corrosive, non-volatile, non-flammable, and non-toxic. These properties are, however, secondary properties which are optimized once a workable system is realized. The primary properties needed for liquid dielectrics from a materials standpoint are discussed here.

A wide liquid phase range in the order of -40 to 100°C is desirable. Although gel systems are being contemplated for study in the future which are not liquid, the present systems require liquidity for function so that Brownian motion can reorient the particles for resettability.

Ability to disperse solid particles is a necessary property for the medium of support. The solution to problems of deficiency in this property can be obtained by several means since ability to disperse is a complex property of substances. For instance, Buscher (1972)[14] has found previously that benzene, even with surfactants, is a very poor dispersing medium. This property is probably related to its low polarizability. Other low molecular weight hydrocarbons in general may be expected to have this problem. The observed facility of carbon tetrachloride as a dispersing medium is related to its large polarizability and accounts in large measure for its present use as a support vehicle. Surfactants can improve the dispersing power of a medium by forming links from the medium which tends to reject particles to the boundary of the

particle. In our magnesium systems the stability of the suspension against flocculation has been greatly enhanced by the use of non-ionic, non-polar surfactants. Dispersibility of particles can also be improved by coating the particles mechanically or chemically before dispersing them. The very favorable dispersing characteristics of aluminum flake pigments is due to the chemically bound layer of stearic acid to the surface of the particles. This layer is essentially a bonded built-in surfactant layer on the particle. Future solutions to dispersing problems will be sought along these lines. As will be discussed in our system analysis sections we feel that a good handle has been obtained for controlling the dispersing of metal particles.

As discussed in Section 2, size and shape of the particles is a transcendent problem for the design of effective phase shift liquids. To the present time we have relied on the commercially manufactured materials while the important factors were being evaluated. As Figure 2-11 shows, the small size distribution region has hardly been touched. In the future, more advanced techniques of small particle reduction must be used. These methods should include sieving, liquid and gas elutriation, and flame spraying. By gas elutriation is meant the process of separating particles using an upward blowing air stream as the sedimentation medium. The flame spraying technique can only be used for those materials which do not burn. Submicron metal particles which are produced by atomization or precipitation techniques may tend to be spheroidal, in which case subsequent comminution may be necessary to flatten the particles for optimizing the shape factor Q.

Chemical stability as a criterion is important for several reasons. The materials themselves must not decompose due either to chemical processes or irradiation by microwaves. Chemical processes such as oxidation can be controlled by several means. For instance, in the aluminum or magnesium particle systems, surface coatings of oxide and surfactants protect the metal against oxidation. The dispersing medium can also be protected against decomposition by introduction of chemical stabilizers. The carbon tetrachloride and carbon tetrabromide systems can be protected against decomposition by adding free radical scavengers such as 1, -6 hexane diamine (Minford et al. 1959)[15]. Such additives also help prevent the attack of the cell walls by the suspension medium. The problem of microwave irradiation stability is fortunately a simple one to solve, since the primary effect of microwave radiation on substances is heating due to dipole absorption process. Since dipolar substances must be rigorously excluded to avoid large insertion losses due to absorption, this problem is taken care of automatically.

An important point concerns the necessity of getting rid of all traces of water in the liquid media. This requirement extends also to the liquid crystal systems. This problem can only be solved by taking great care in the procurement and preparation of the liquid systems.

Another difficulty can arise from the presence of small amounts of ionic materials in the various compounds. These ionic materials can cause losses in the efficiency of the bias field in producing a polarization in the liquid phaser medium. Again care in purification of the systems can take care of a majority of the problem.

5.2 GENERAL CONSIDERATIONS OF PHASE SHIFTING REQUIREMENTS

Section 2 discusses in a theoretical way the requirements for good phase shifting liquid systems which are composed of metal particles suspended in liquids. The general requirements which apply also to other systems such as ferroelectric fluids and liquid crystals are easily abstracted from the theory. For good phase shifting ability large, highly asymmetric molecules or particles with large polarizabilities are required. The particles can also have a large, intrinsic permanent dipole moment if it is directed along the longest axes of the molecule. Permanent dipole moment components directed along short axes of the molecule will enable dipole absorption to take place in the microwave region. The solvating medium if present must be non-polar or dipole absorption process will take place. The two requirements just mentioned preclude, unfortunately, the use of large protein molecules with huge dipole moments because high dielectric constant solvents are necessary to dissolve them in a way to get maximum Kerr effect. Such high dielectric constant solvents always have large dipole moments. A case in point is the observation that poly benzyl-l-glutamate, PBLG, has a high optical Kerr constant when dissolved in ethylene dichloride but a low optical Kerr constant when dissolved in dichloroacetic acid [16]. The general conclusion can be made that high dipole moment structures are stabilized by high dielectric constant media with large dipole moment.

5.3 METAL PARTICULATE SYSTEMS

5.3.1 SOURCE OF PHASE SHIFT CHARACTERISTICS

The source of the phase shift characteristic is the macroscopic orientation of disc-like particles of dimension ~1-10μ by an applied electric field. The orientation is produced by dipole induction torques. Relaxation is caused by Brownian motion in the fluid.

5.3.2 CURRENT CAPABILITIES

The S-Band capabilities of metal particulate systems are listed in Table 5-1. It may be noted that the Mg:CCl_4:CBr_4 system is stable enough for applications which do not require fast response times.

Table 5-1. Metal Particulate System Capabilities at S-Band

System	Al:CCl_4	Mg:CCl_4:CBr_4
Total Phase Shift (Low Power Tests)	0- 360°/0-200V	0-100°/0-500V
Loading Density	10 mg/cm^3	10 mg/cm^3
Low Field Strength Response Time (< 200V/cm)	5 sec	5 sec
Resettability	5° @ 360°	
Insertion Loss	0.5 dB	0.7 dB (with Tergitol)
Temperature Coefficient	1.5°/°C @ 360°	
Dielectric Constant	2.5 @ 100 kc	
Power Level	1 MW peak; 1 kW avg	1 MW peak; 1 kW avg

5.3.3 SYSTEM DESCRIPTION

Two metal particulate systems which have been studied:

1. Al:CCl_4, aluminum flakes 1-10μ suspended in CCl_4, no flocculation, settling time 10-15 min
2. Mg:CCl_4:CBr_4, magnesium particles ~10-20μ suspended in mixture of CCl_4 + CBr_4 with density of 1.79 gm/cm^3. Tergitol prevents flocculation; settling time ∞.

5.3.4 METHOD OF MANUFACTURE

Industrially available metal powders were taken and suspended by agitation in the fluid medium; see Table 5-2. For any pastes used the physical cleaning of the stearic acid binder was performed by dissolving the paste binder in some organic solvent (CCl_4, CH_2Cl_2, $(CH_3)_2CO$). Then the resultant powder was suspended in the fluid. Tergitol was added to the magnesium systems. The surfactant was bound to the particles by boiling the liquid mixture under reduced pressure in a warm water bath.

The carbon tetrabromide commercially obtained was of technical grade and quite impure. This compound was purified by recrystallizing from ether several times. Once pure CBr_4 was obtained the solutions with CCl_4 and mixtures with Mg were stable in the dark. When traces of moisture were present some debromination occurred

Table 5-2. Currently Used Metal Particles

Metal	Name	Manufacturer	Solvent Density, gm/cc
Al	XD-40	Reynolds	1.6 CCl_4
Al	"AA"	Silberline	1.6 CCl_4
Mg	RMC-325	Reade	1.8 CCl_4-CBr_4

in the presence of light. Rigorous exclusion of water prevented this problem. The density range available from 10°-40°C with CCl_4-CBr_4 mixtures were found to be 1.6-2.1 gm/cm^3.

Problem Areas

The aluminum systems are not stable for more than 15 minutes because of the high density of the particles with respect to the dispersing solvent (Al, $\rho = 2.71$ gm/cc and CCl_4, $\rho = 1.59$). We are not able at present to manufacture a density matched medium unless the temperature of operation of the cell is above 40°C. As a result of settling pumping must be used to keep the particles suspended. However, efficient pumping usually results in up to a 50-95% decrease in the phase shift ability. The magnesium systems are stable to settling, and the flocculation problem can be cured by binding a surfactant as mentioned previously. The problem with current Mg systems is that they show a phase shift ability of 50% of the Al systems.

Because the aluminum particles tend to "paint" or coat the interior of the waveguide there is a tendency for breakdown to occur. This does not seem to be a problem in the magnesium system.

5.3.5 PROSPECTS

Unless a density matched liquid is found for the Al systems these systems do not seem to have a bright future. However, if a method of producing and handling particles in the order of 0.01-0.05μ can be found, then the systems would be feasible. Aluminum has the useful property that it easily forms highly assymetric flakes which have excellent phase shift characteristics. If possible this property ought to be used. The same considerations apply to the magnesium systems. In addition, submicron metal particles improve several other areas too. For instance, the necessity of using CCl_4 and CBr_4 as dispersing media can be eliminated and such inert and non-toxic materials as fluorocarbons can be used as dispersing media when the particle size is on the order of 0.01μ. Also the elimination of CCl_4 and CBr_4 means that other metals, perhaps of better flakeability, can be used.

The use of other solvents may well eliminate the problem of aluminum painting. Smaller particle size of course, means that the goal of microsecond set and preset times can be obtained with low applied bias voltage.

5.4 LIQUID CRYSTAL SYSTEMS

5.4.1 SOURCE OF POSSIBLE PHASE SHIFT CHARACTERISTIC

Phase shift is attained in these systems by electric field or magnetic field induced anisotropy of the dielectric constant due to the reorientation of structural domains in the bulk liquid. The reorientation can be achieved by dipole induction of the domains or dipole orientation of the domains.

5.4.2 CURRENT CAPABILITIES AND RESULTS

So far in the systems studied no detectable phase shift has been observed. The systems studied fall into several categories as shown in Table 5-3.

5.4.3 PROBLEM AREAS AND PROSPECTS

There are several problem areas in the current liquid crystal research program. The first area is due to the microwave absorption by many liquid crystals. Those molecules with off axis dipoles tend to absorb in the microwave. The next problem is obtaining liquid crystal systems which have their nematic or cholesteric phase region over a convenient range of temperature, including the range of 15-40°C. This problem seems related empirically to the first, in that the available low temperature systems seem to require an off axis dipole moment. This is probably related to the fact that low temperature ranges are facilitated by bulky off axis groups which often have dipole moments. The prospects for these systems seem fair and depend on the availability of new liquid crystal systems. The systems which have been tested were primarily solution systems because the substances themselves all had high melting temperatures. New liquid crystals are now becoming available which should enable more investigation to take place.

One other possible problem area is that orientation due to electric fields seems to require a field intensity of ~10000 v/cm which is a fairly large bias for electrode spacings of 1 cm. So far pulse experiments with the cholesteric systems have not yielded positive results, because the duty cycle of the pulse unit (~25%) is not enough.

We have continued the search for appropriate components that have no off axis dipole moment and are liquid in a reasonable range. This requirement may well be obtained by using mixtures of liquid crystals especially cholesteric-nematic mixtures which seem to have low nematic phase ranges. Meier and Saupe[17] have established that the microwave dielectric constant can be significantly changed by magnetic fields in p-p' azoxyanisole.

Table 5-3. Liquid Crystal Systems

	Solvent	Insertion Loss/19 cm @ Ku-Band
A. SOLUTIONS OF NEMATIC CRYSTALS		
10% N-p-methoxy benzylidene p-butyl aniline	C_6H_{12}	20 dB
12% p-p azoxy diphenetole	CCl_4	0 dB
12% p'-p (ethoxy phenyl azo) phenyl undecrate	CCl_4	4 dB
11% butyl p-(p-ethoxy phenoxy-carbonyl phenyl carbonate)	CCl_4	3.2 dB
B. SOLUTIONS OF CHOLESTRIC CRYSTALS		
17% Cholesteryl 2-ethyl hexonoate	CCl_4	1.5 dB
C. NEAT NEMATIC CRYSTALS		
N-pmethoxy benzylidene p-butyl aniline	-----	>40 dB
D. NEAT CHOLESTERIC CRYSTALS		
Eastman 922165 Cholesteric Mixture	-----	20 dB

5.5 FERRO-FLUID SYSTEMS

5.5.1 SOURCE OF PHASE SHIFTING CHARACTERISTICS

Sub micron particles with either permanent electric or magnetic moments are oriented by either electric or magnetic bias fields. If the particles are asymmetrical or have anisotropic principal polarizabilities then the bulk medium should exhibit anisotropy of the propagation velocity, $v = (\sqrt{\epsilon \mu})^{-1/2}$. Fluids made up of ferroelectric particles would be called ferroelectric fluids, while these made up of ferromagnetic particles would be called ferromagnetic fluids.

5.5.2 PROSPECTS

Ferrofluidic Corporation has demonstrated the feasibility of manufacturing ferromagnetic fluids. We have tested a sample of their material HO1 in the Ku-band cell which had 1000 amp turns over 19 cm. A phase shift of ~150° was observed, demonstrating the feasibility of this material as a phase shift substance. Ferroelectric fluids constructed from ferroelectric particles such as titanates should exhibit similar characteristics under orienting electric fields. Such systems should be stable suspensions in inert, non-toxic perfluorocarbon bases with rapid set and reset times. These systems should have a bright future.

5.6 PROTEIN SOLUTION SYSTEMS

5.6.1 SOURCE OF PHASE SHIFTING CHARACTERISTICS

Several well known proteins have very large dipole moments and are quite anisotropic,[18,19]. Protein systems have been a valuable area for research in optical Kerr effect studies. The phase shift ability arises from two sources. These proteins have large permanent moments which can be oriented by a bias field. If the particles are asymmetric they will present variable optical thicknesses to the transmitted beam. In addition, these molecules are relatively polarizable so that the induced moments can be oriented by the field, (O'Konski, 1972)[19].

5.6.2 PROSPECTS

As mentioned in 5-2, protein molecules with large dipole moments require high dielectric constant solvents to stabilize them for large Kerr effects. Unfortunately, these solvents absorb strongly in the microwave region because they have dipole moments. As a check we have examined at Ku-band the insertion losses of several high dielectric constant solvents which are found in Table 5-4. None of these solvents had transmission at Ku-band as predicted. In Table 5-5 are some literature values for the loss tangent at 10 GHz for some solvents. Table 5-6 lists several proposed systems of proteins and solvents which on the basis of the known absorptions of the solvent must be rejected as possible phase shift systems.

Table 5-4. Measured Insertion Losses for Some Solvents at Ku-Band

Solvent	Insertion Loss	Dielectric Constant
Dichloro methane	20 dB/19 cm	9.1
1, 2 Dichloro ethylene	26 dB/19 cm	9.2
1, 1, 1 Trichloro ethylene	22 dB/19 cm	3.4
1, 1, 2, 2 Tetra bromo ethylene	30 dB/19 cm	7.0

Table 5-5. Loss Tangents for Some Solvents at 10 GHz*

Solvent	Tan δ
Water	5400×10^{-4}
Ethanol	680
Propanol	900

*A. Von Hippel, "Dielectric Materials and Applications", Wiley N.Y., N.Y. (1954)

Table 5-6. Some Proposed Phase Shifting Protein Systems

Protein	Solvent
1. Carboxy Hemoglobin	Water
2. Edistin	Water
3. Gliabin	Water
4. Gamma Serum Pseudo Globin	Water
5. Zein	Water + Propanal
6. Zein	Water + Ethanol
7. B-Lactoglobulin	Glycine (melting point 262°C)
8. B-Lactoglobulin	Water + Glycine

6. PERMITTIVITY TESTS

6.1 DIELECTRIC TEST CELL

One of the major problems encountered working with the liquid phase shifter was evaluation of the artificial liquid dielectric constant. Batch preparation was a long, tedious operation and no simple method existed to study the preparation. Eventually a test procedure was developed to evaluate some of the dielectric properties in a more easily controlled environment by using a capacitance test cell to observe directly any changes in the dielectric constant. The capacitance of a test cell in a dielectric can be described by the relationship:

$$C = \epsilon_r(E)\, C_o \qquad (6\text{-}1)$$

where C_o is the capacitance when $\epsilon_r = 1$ (in air), and $\epsilon_r(E)$ is the dielectric constant as a function of the applied field strength. With this test cell it was possible to observe directly the effects of flow, ac, and dc applied fields, concentration and particle size on the permittivity and the ability of the permittivity to change.

6.2 CELL CONSTRUCTION AND TEST SET UP

A number of test cells were constructed to investigate various properties of the liquid dielectric. All had plate areas of approximately 25cm^2 and the separation of electrodes was 1cm. The electrodes were fabricated from the copper-clad material. A number of configurations were employed, depending on the parameter then under study. Capacitance was measured as shown in Figure 6-1. The major difficulty encountered using this particular capacitance bridge was that ac fields could not be directly used and only dc measurements were made.

6.3 PERMITTIVITY VS. CONCENTRATION

One of the initial drawbacks in determining batch-to-batch reproducibility of the Al-CCl_4 liquid dielectric was that no means existed of non-destructively determining the concentrations of the liquids. While it is difficult to determine a priori what the behavior of a particular conducting paste will be without some idea as to the number densities and particle distribution, some indications can be anticipated. Assuming no interactions between dipoles within the dielectric, which would seem a reasonable assumption up to moderate densities, the addition of more conductors to a liquid dielectric should be a linear function; that, is the change in dielectric constant $\Delta\epsilon'$

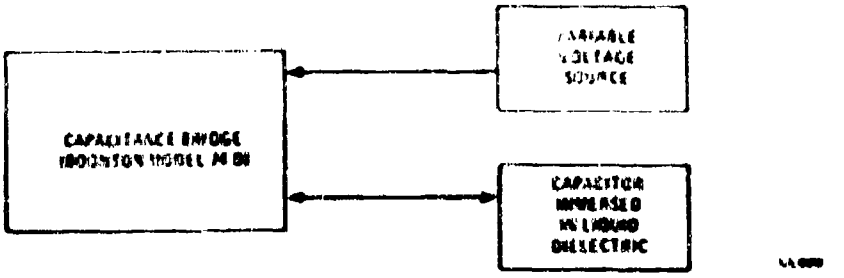

Figure 6-1. Capacitance Test Cell to Measure Permittivity With Changes in Applied Voltage

should approximately double with addition of twice as many particles to a solution. These assumptions agree very well with experimental data. Plots of dielectric constants vs. applied electric field were made on the capacitance test cell for various concentrations of aluminum using a non-insulating electrode and a dc applied field, Figure 6-2, were used as a standard to calibrate unknown samples. Comparison with magnesium is shown in Figure 6-3.

For the S-band cell, it has been calculated that a change of ϵ_r of .5 was necessary for 360° phase shift. One can see that at lower densities (< 10 mgm/cc) this would only be possible by going to larger field strengths (that is, > 400 volts/cm). However, going to larger fields is no guarantee of more permittivity change, as saturation may be reached.

The reason these curves were not expanded to higher densities is due to increased settling of the aluminum, and increased difficulty in measurements.

6.4 LONG TERM D.C. VOLTAGE EFFECTS

At higher densities (>20 mg/cc) a peculiar effect is observed with Silberline "AA" in the test cell; see Figure 6-4. There is a large increase in the capacitance (ϵ_r) followed by an abrupt decrease. This effect becomes more pronounced at higher densities and only seems to appear in the case of a dc field. It was first felt that this effect might be caused by shorting between the non-insulated electrode, but no current was observed. What may be responsible is that as the density increases, the interparticle distance decreases and that dipole-dipole interactions between particles occurs. As the bias field is applied, the particles initially align, then the dipole-dipole interactions set in. This results in a dealignment until the particles find themselves in a more favorable energy state. Possibly this demonstrates inertial effects in orientation.

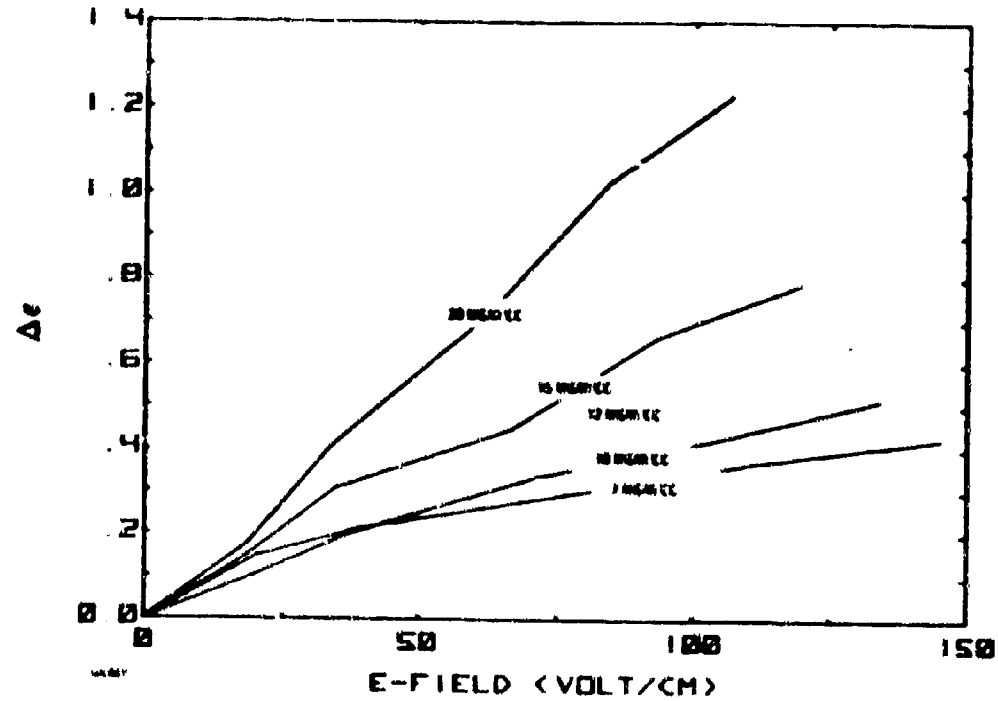

Figure 6-2. Change in Permittivity for Various Particle Loading Densities of Silberline "AA" Aluminum

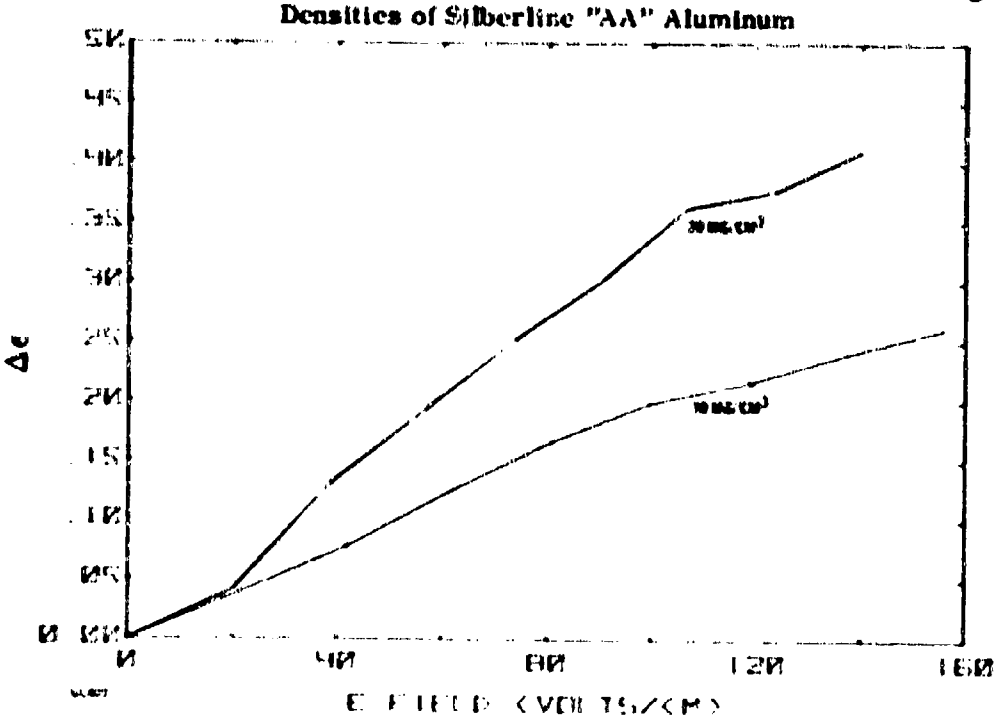

Figure 6-3. Change in Permittivity for Two Particle Loading Densities of Magnesium Powder, Reade 325-X

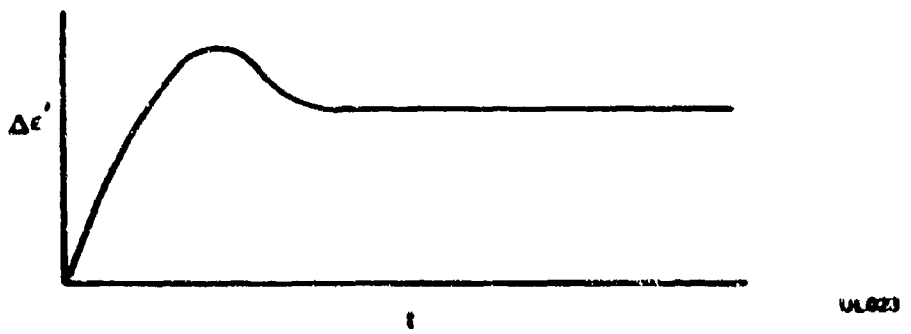

Figure 6–4. High Field Strength Overshoot in Permittivity Change vs. Time for Particle Densities Greater than 20 mg/cc

7. LOW POWER TESTING

A series of tests was run to prepare comprehensive data curves indicating microwave performance characteristics of the liquid phase shifter. These tests, schematics of test set ups, results, comparison to theory, and interpretations are organized here.

7.1 INSERTION LOSS, ELECTRODE DESIGN

A number of tests were performed on the phase shift cell employing different electrode configurations to examine cell loss characteristics. Figure 7-1. Initially, the S-band phase shift cell employed a single electrode design, as did the K_u-band cell. To insure homogeneity of the liquid dielectric material, holes were drilled through the electrode at randomly chosen positions. It was observed that the hole size affected the insertion loss. The results for a single electrode phase shift cell with various hole sizes employing a CCl_4 dielectric ($\epsilon_r = 2.17$) is shown in Figure 7-2. For comparison purposes an insertion loss measurement of the phase shift cell filled with carbon tetrachloride but without the electrode and electrode supports was made, see Figure 7-3. For this and all other measurement the teflon impedance matching wedges are in place. The average insertion loss over the band from 2.7 to 2.9 GHz is 0.12 dB.

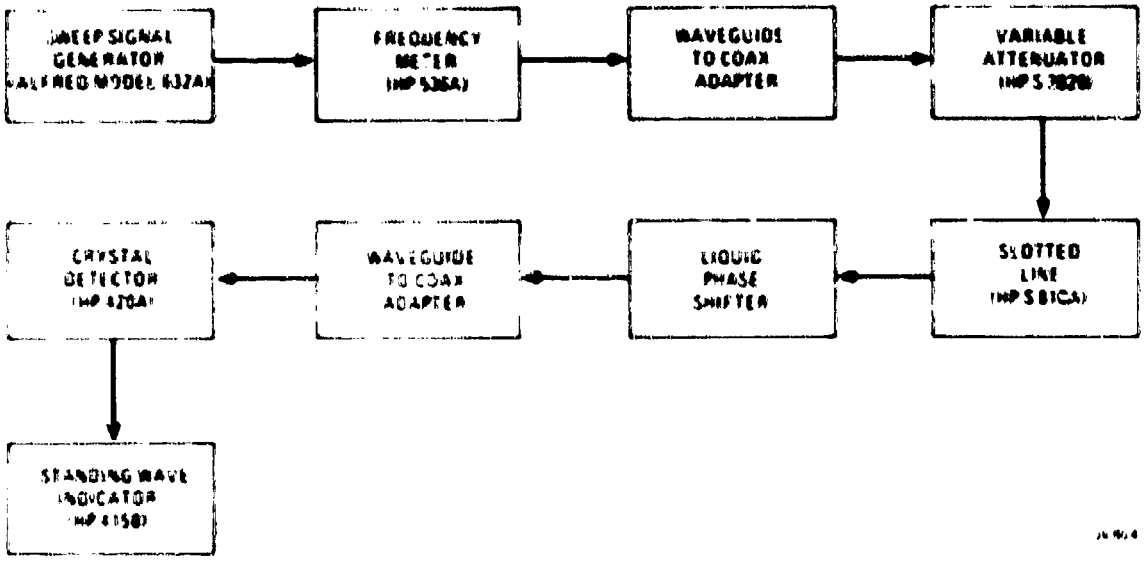

Figure 7-1. Insertion Loss Test Setup

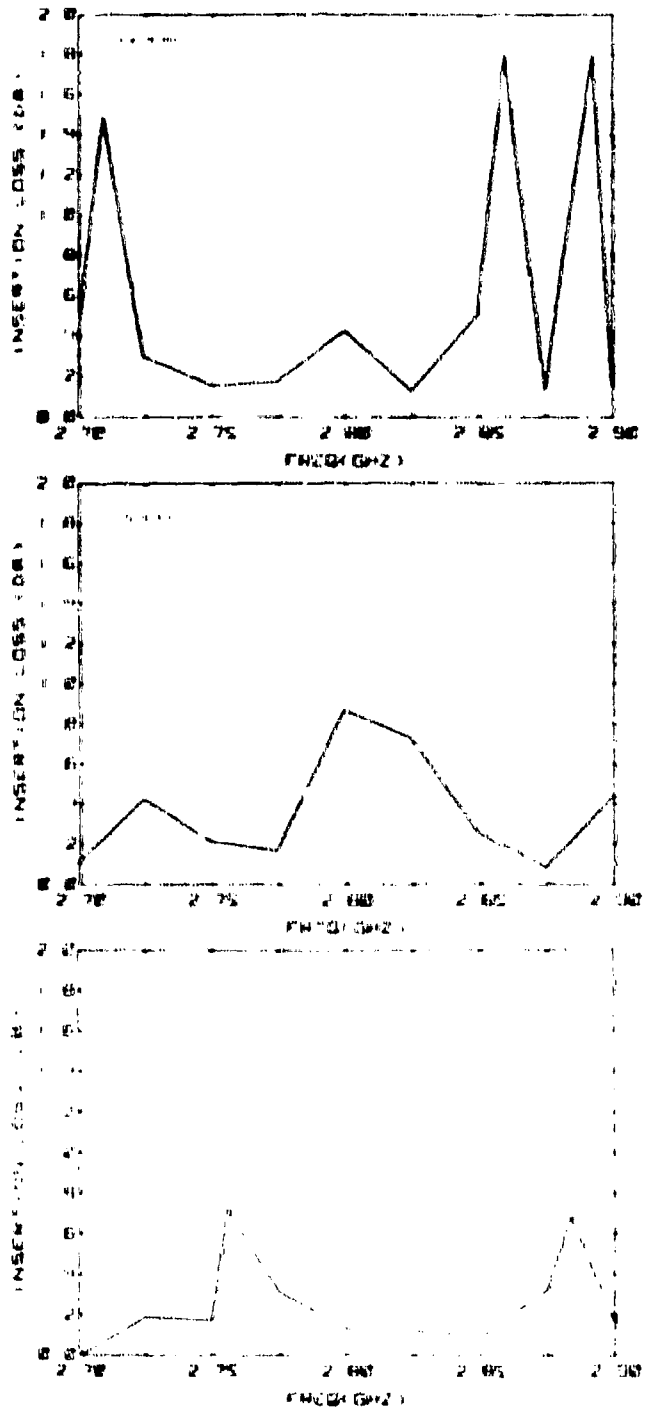

Figure 7-2. Insertion Loss vs. Frequency for Single Electrode Phase Shifter for Various Hole Sizes with CCl_4

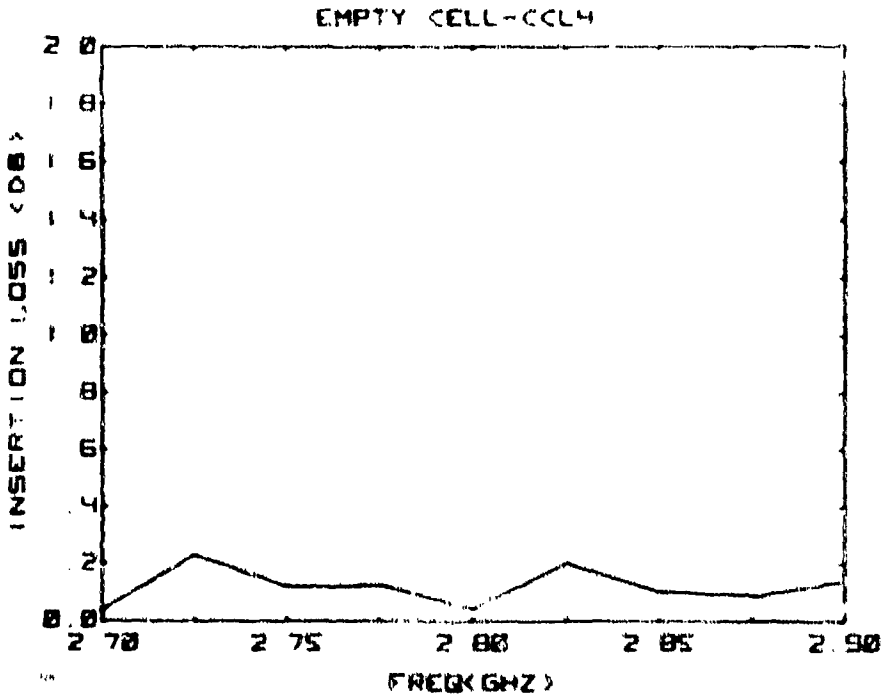

Figure 7-3. Insertion Loss vs. Frequency for Phase Shift Cell Without Electrode and Filled with Carbon Tetrachloride

The trend seems to be that the larger the hole size, the smaller the insertion loss peaks. Each single electrode examined was exactly the same length and had the same number and placement of holes (except for their diameter). The insertion loss peak phenomenon was investigated extensively and can be explained as being caused by higher order evanescent modes, initiated at the electrode edge. (Further account of this is given in Section 3.) The pentaplate was designed because it is desirable to work with the lowest possible phase shifter control voltage. The insertion loss for the pentaplate configuration was measured for the cell filled with CCl_4 ($\epsilon_r = 2.17$, Figure 7-4) and Al-CCl_4 ($\epsilon_r = 2.35$, Figure 7-5) over the band from 2.7 to 2.9 GHz. Comparison of the pentaplate and single electrode configurations shows no insertion loss peaks, which would indicate no lossy evanescent modes (no higher order modes were ever measured).

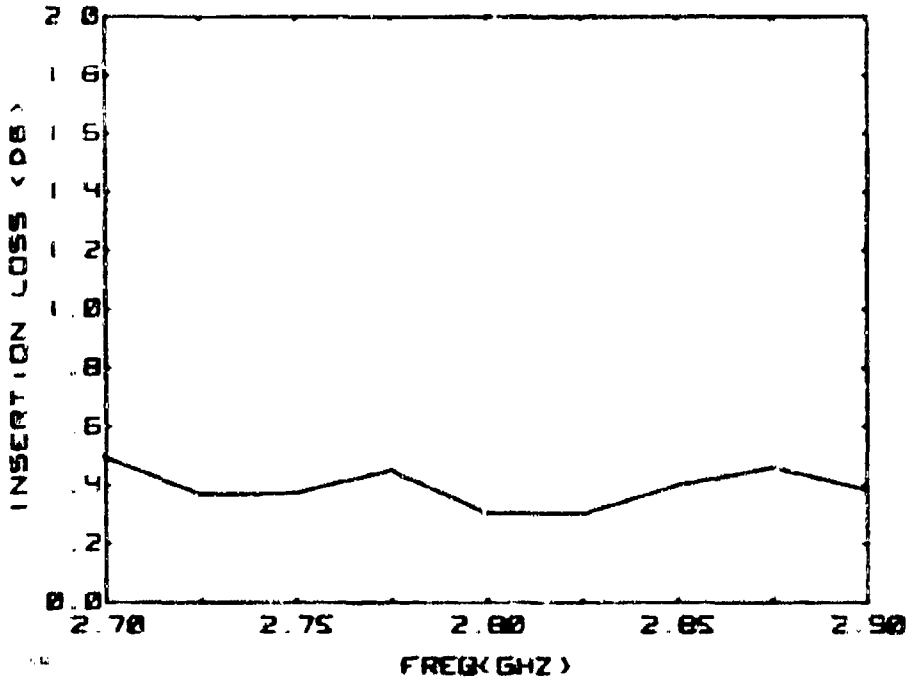

Figure 7-4. Insertion Loss for Pentaplate Electrode with CCl_4

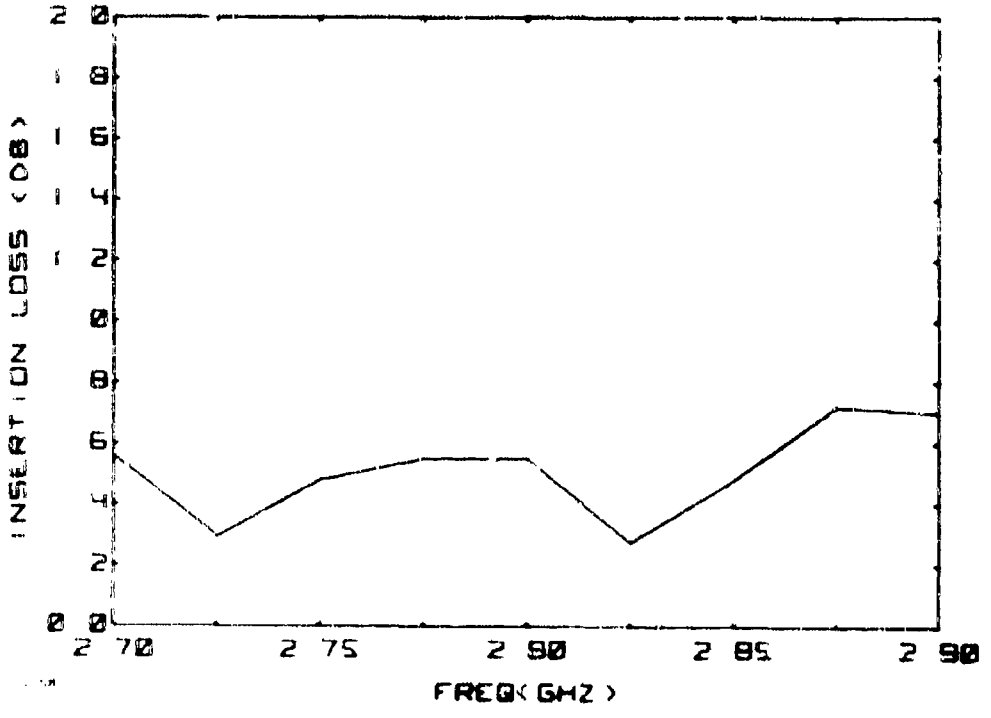

Figure 7-5. Insertion Loss of Complete Pentaplate Phase Shifter with CCl_4 and Al

Examination of the data from the phase shift cell filled with Al-CCl_4 shows that it is somewhat more lossy than the pure dielectric case. The increased losses in the Al-CCl_4 system can be explained by:

1. Mismatch between impedance wedges ($\epsilon_r \simeq 2.1$) and the Al-CCl_4 artificial dielectric liquid ($\epsilon_r \simeq 2.35$): see Section 3
2. The matching condition (equation 3-12) was not being met exactly, spacing between the discontinuities of the electrode, which is dependent on ϵ_r, was not exact for this particular liquid
3. Losses due to the presence of the aluminum conductor.

7.2 VSWR, ELECTRODE DESIGN

As in the case of the insertion loss, the VSWR, as shown in Figure 7-6, was investigated for both single and pentaplate electrode configurations. Results are shown in Figure 7-7, and 7-8. The measured VSWR data for the pentaplate electrode, Figure 7-9, compare favorably with those of the single electrode.

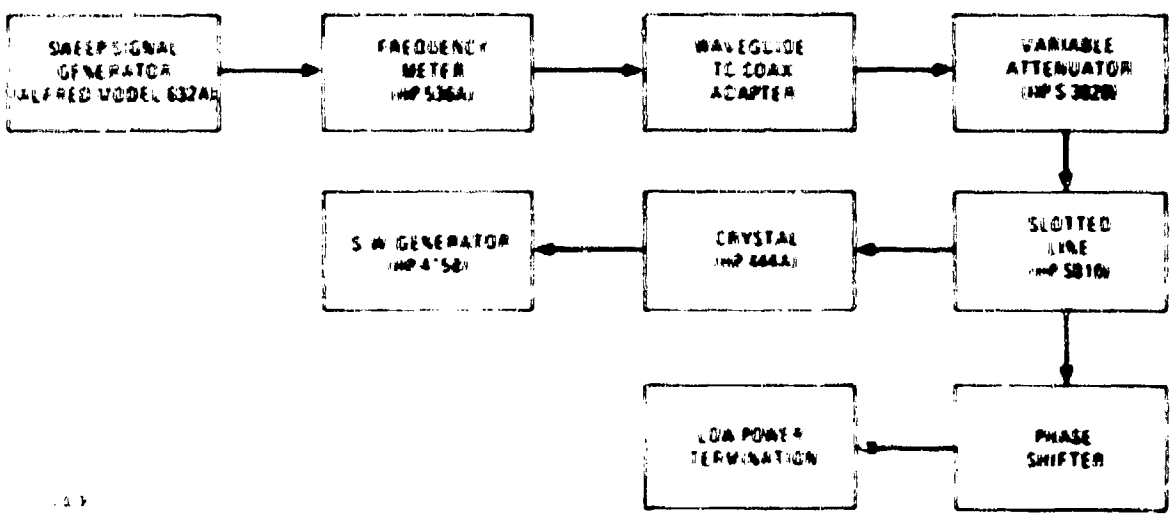

Figure 7-6. VSWR Test Setup

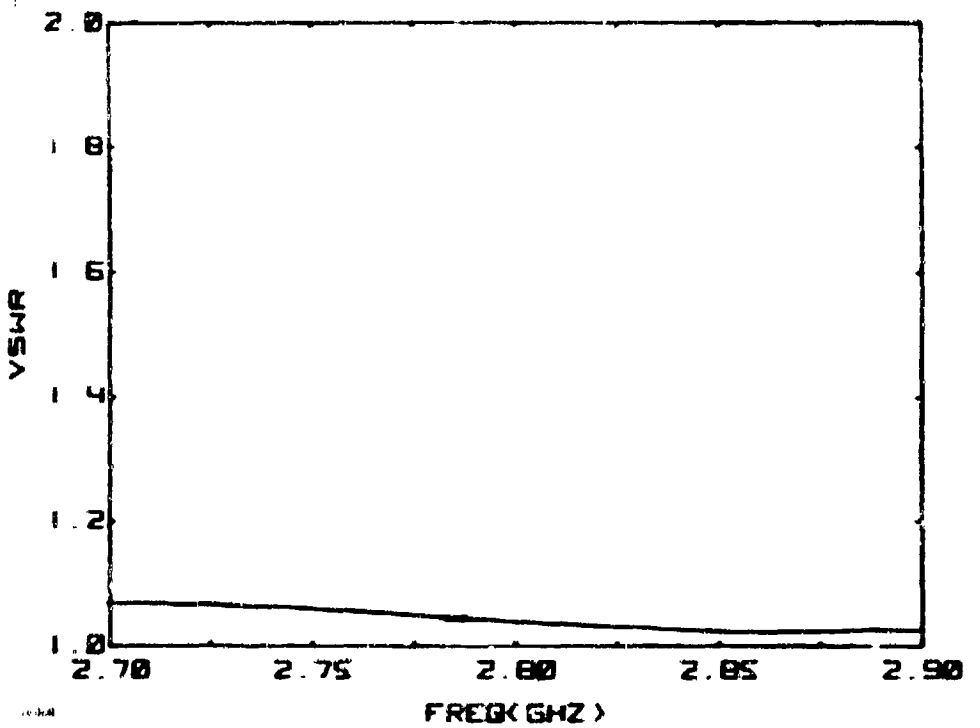

Figure 7-7. VSWR vs. Frequency for Phase Shift Cell Without Electrode and Filled with Carbon Tetrachloride

7.3 PHASE SHIFT VS. CONTROL VOLTAGE

A significant portion of the effort spent on the phase shifter has been devoted to this facet of the investigation using the setup shown in Figure 7-10. Examinations were made not only with different electrode configurations but also with different materials.

7.3.1 ELECTRODE CONFIGURATION

In Section 3, a discussion and comparison of the single and pentaplate electrode configurations was given. Test results are given in Figure 7-11. The single electrode data is for a 58 cm electrode using an Al-CCl_4 artificial dielectric. The pentaplate data was taken using the same artificial dielectric, however, the electrode was only 44 cm long. Thus, the really important difference between the two configurations is the efficiency of the electrodes, that is, the phase-shift-per-unit-length of the two configurations, shown in Figure 3-4. Because of this larger phase-shift-per-unit-length of the pentaplate electrode configuration, not to mention the lower insertion loss and VSWR, it was the preferred configuration and employed in all subsequent testing.

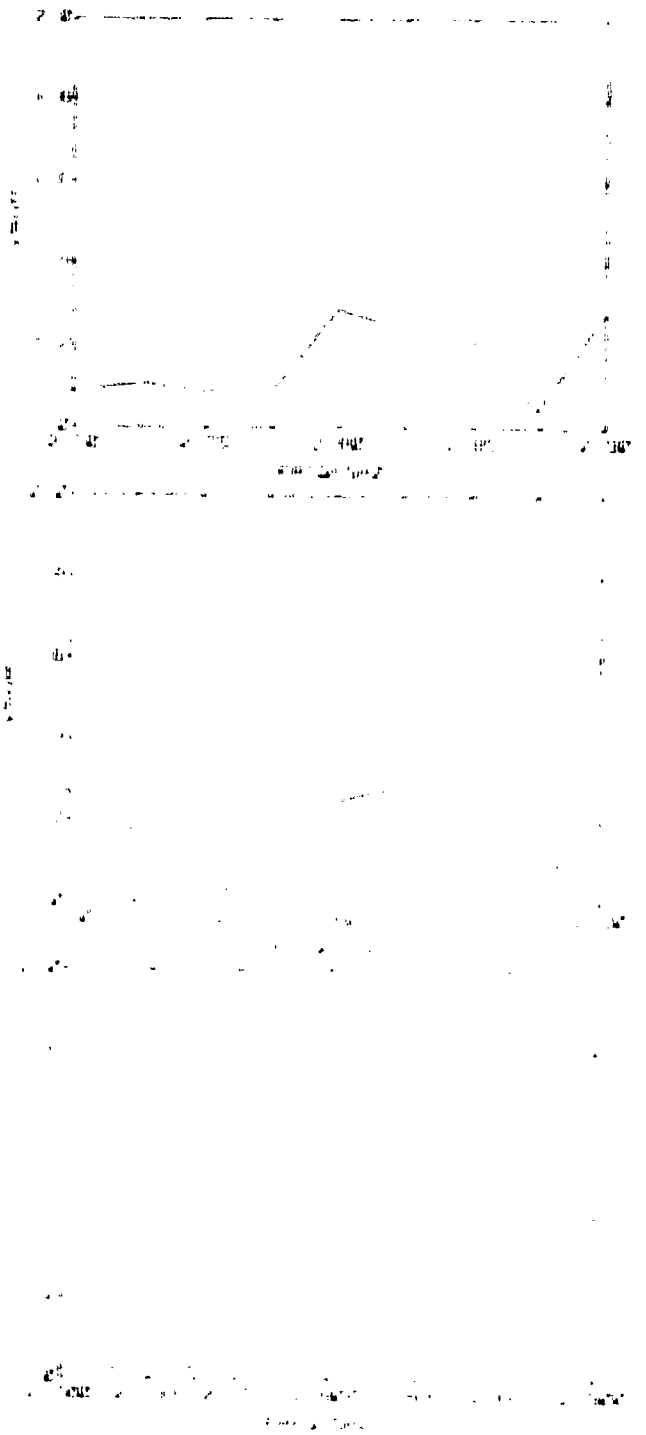

Figure 7-8. VSWR vs. Frequency for Single Electrode Phase Shifter for Various Hole Sizes

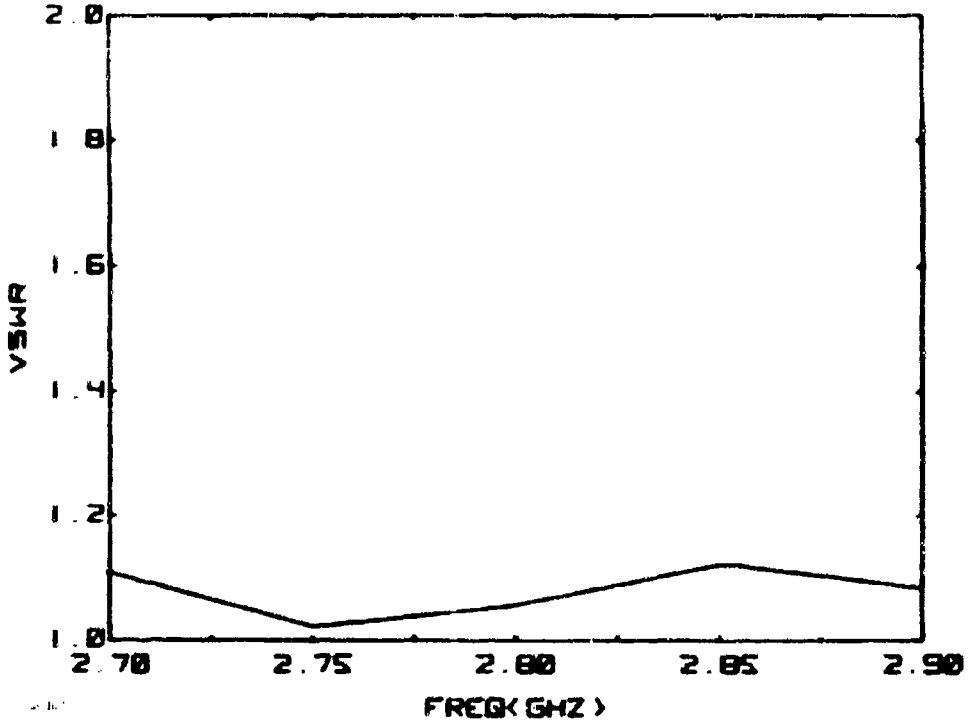

Figure 7-9. VSWR of Pentaplate Electrode with Carbon Tetrachloride

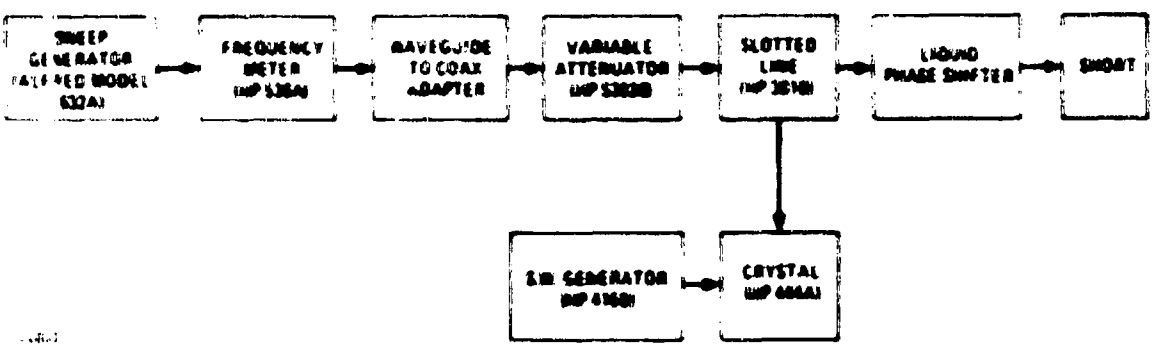

Figure 7-10. Phase Shift Measurements Test Setup

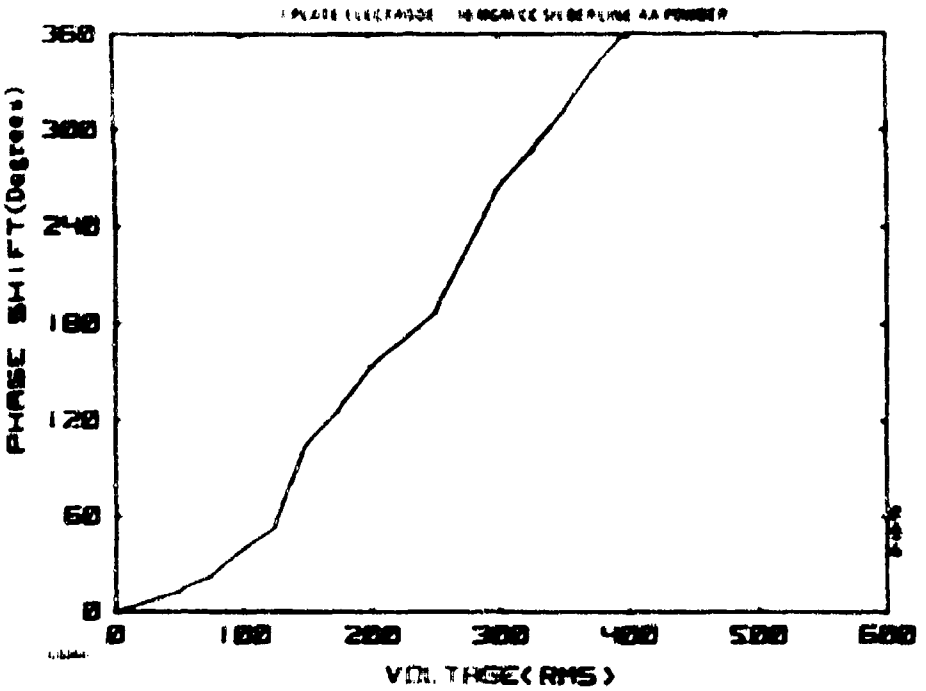

Single Plate Electrode, 58 cm

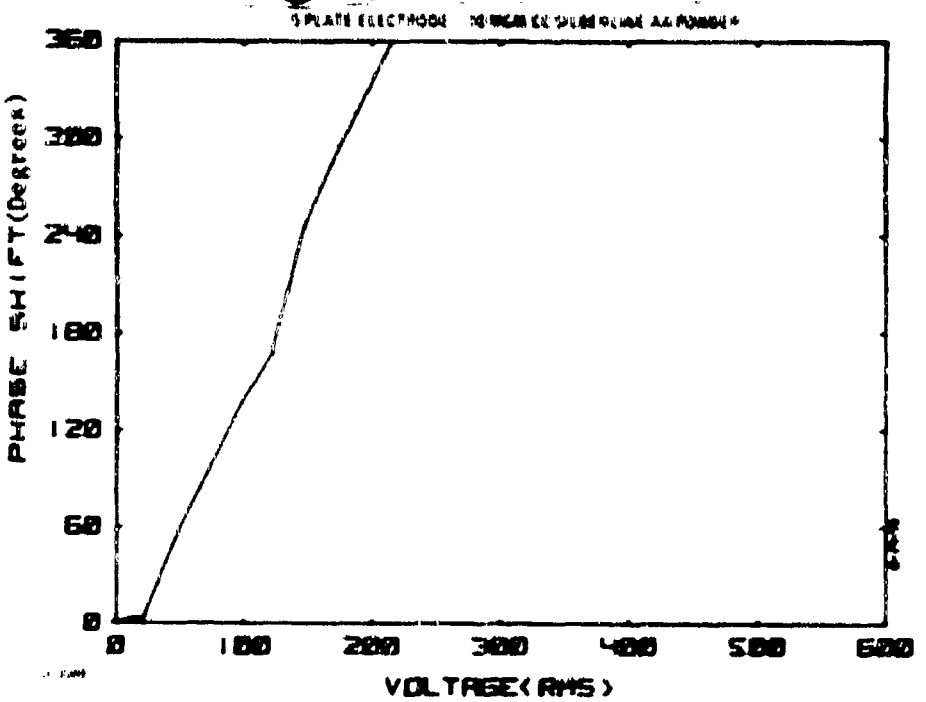

Pentaplate Electrode, 44 cm

Figure 7-11. Phase Shift vs. Applied Voltage with Silberline "AA" Aluminum in Cell

7.3.2 Al-CCl_4 MATERIALS TESTING

The major problem with the Al-CCl_4 artificial dielectrics lay in problems of settling and coating, yet, it remained the most successful material developed in terms of maximum producible phase shift. Investigations were run in the S-band system comparing two different aluminum brands; results are shown in Figure 7-12. Some aluminum preparations seemed to work better (i.e. provide more phase shift for a given voltage) than others, which can be attributed to different asymmetries and particle size distributions. From theoretical considerations, the larger particle (which would have larger polarizabilities) would saturate at lower field intensities. Thus, one would expect that the preparations with the smallest amount of phase shift at peak recorded E field are those preparations with the smallest particles. It would be these particles that one would expect would have faster rise and fall times. Unfortunately, due to the instability of Al-CCl_4 preparations, this point never could be investigated in depth.

Tests were also conducted varying the density of the aluminum added to the CCl_4 dielectric. Variation in density tests were performed for different aluminum preparations in the dielectric test cell and compared favorably with theory. Tests run in the K_u-band phase shift cell, Figure 7-13, agreed with the findings of the dielectric test cell. Gross details in phase shift were possible but measurement errors due to settling and coating of the aluminum (after pumping was stopped) were probably on the order of 10% with the Al powders and pastes.

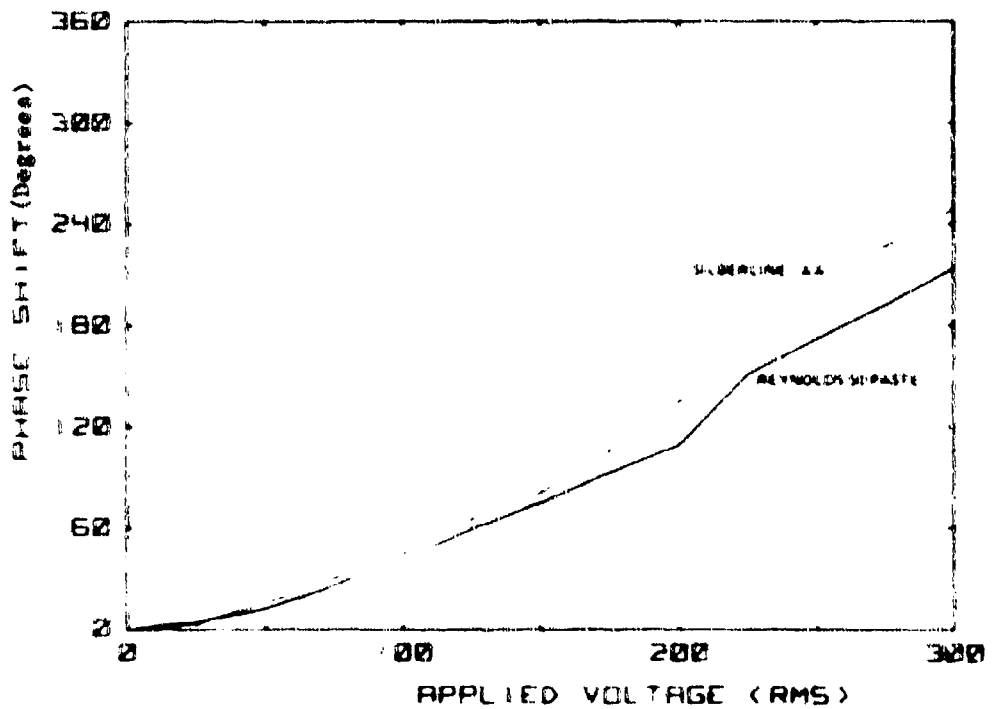

Figure 7-12. Obtainable Phase Shift with Silberline Powder and Reynolds Paste Aluminum at S-Band

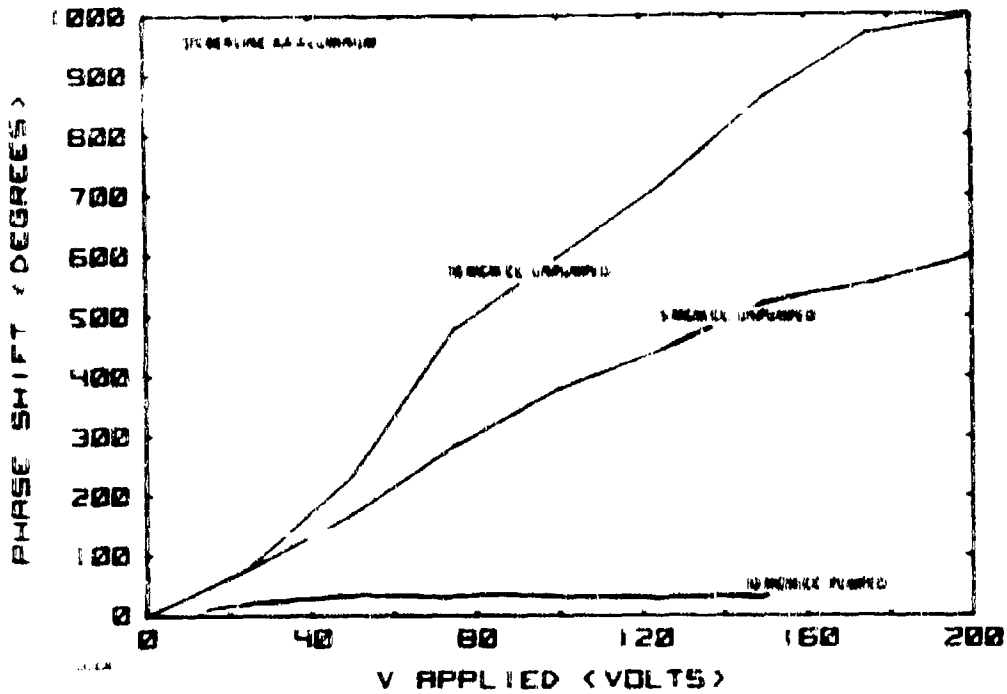

Figure 7-13. K_u-Band Phase Shift with Various Densities of Silberline "AA"

7.3.3 Mg - CCl_4-CBr_4 MATERIALS TESTING

In the search to find a more stable liquid, the Mg : CCl_4 : CBr_4 density matched system was developed as described in Section 6. The advantage of this system is that settling and coating problems are minimized, although some flocculation has been observed. This problem, though, seems to be related to trace amounts of water present in the system and can be remedied by use of the proper surfactant to wet the magnesium. Test results at various frequencies and densities are shown in Figure 7-14. There is not as great a skew in the data as with aluminum, due to the increased stability of the system. However, one of the disappointments in the magnesium system lay in the fact that ~180° phase shift seemed to be the limiting phase shift value at saturation for the same loading density as has been used for aluminum. This is probably so because the aluminum particles are more platelike and smaller than the available 325 and 400 sieve magnesium and therefore have a much larger number density than the magnesium particles. It is important to note that magnesium approached a saturation level much faster than the aluminum particles, indicating that the greater portion of magnesium particles were probably much larger than the aluminum particles. One would expect then, that the corresponding number density of magnesium particles as opposed to aluminum particles would be considerably less, thus the smaller limiting value in the case of the magnesium artificial dielectric.

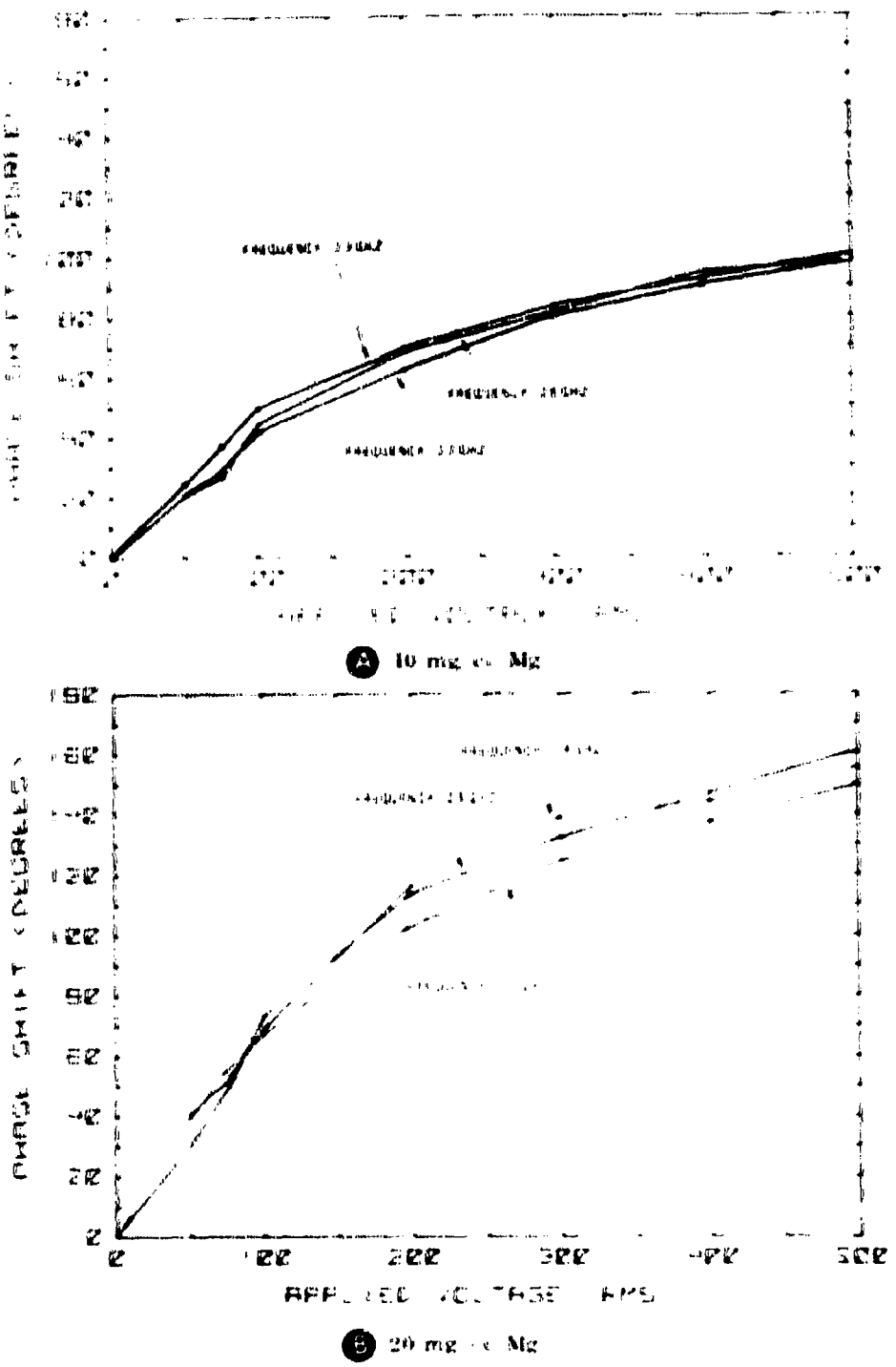

Figure 7-14. Phase Shift vs. Applied Voltage for Mg-CCl_4-CBr_4 Dielectric at Various Frequencies and Densities

7.3.4 DISPERSION OF PHASE SHIFT

Tests were conducted investigating phase shift vs. applied voltage for various wavelengths across the band of 2.7-2.9 GHz for both the Al-CCl_4 and Mg-CCl_4-CBr_4 dielectric. Unfortunately, in the case of the Al-CCl_4 dielectric, the data is not consistent (Figure 7-15). This, however, was attributed to particle settling over the 8-hour period of testing and coating of the electrode by the preparations, which probably limited measurements to an accuracy of 10%. Normally, without particle settling one expects increased amount of phase shift as the RF frequency is increased.

Testing was much more successful in the case of the Mg-CCl_4-CBr_4 liquid dielectric. The dispersion curves (Figure 7-14) are very close to the expected $1/\lambda$ behavior and are at least consistent and in the proper order.

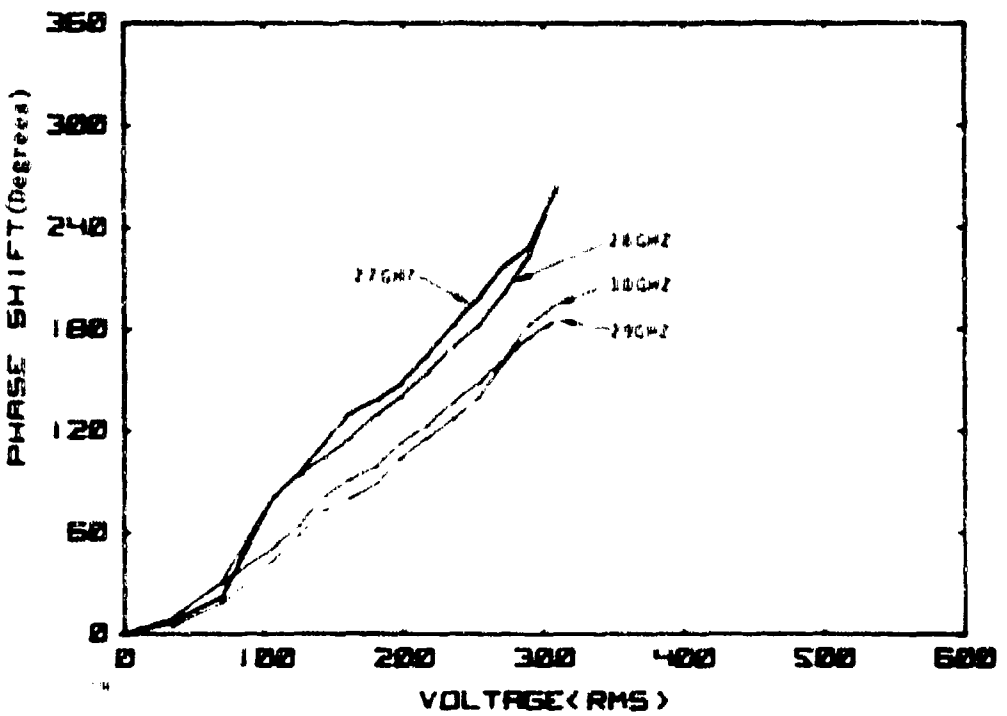

Figure 7-15. Phase Shift vs. Applied Voltage Showing Effect of Phase Shift Dependence on Frequency

8. HIGH POWER TESTS

One of the objectives of this feasibility study is a demonstration of the high power handling capability of the phase shifter. The Electronics Division procured a transmitter and established a 500 sq ft high power test laboratory to evaluate the high power handling capability of the phase shifter and components of other radar systems in production.

The building blocks of the high power test laboratory, made up from both the FPS-6 and FPS-18 radar systems are:

Transmitter, Radar	T-338/FPS-6
Modulator Group	OA-329/FPS-6
Power Supply	PP-783/FPS-6
Voltage Regulator	CN-93/CPS-6B
Heat Exchanger	MX-2010/FPS-18

The operating characteristics of the transmitter are:

Operating Frequency	2.7935 GHz
Pulse Width	2 microsec
Pulse Repetition Frequency	360
Duty Cycle	0.00072
Peak Power Output	5 Mw
Average Power Output	3.6 kw

The equipment setup for high power testing is shown in Figure 8-1, all waveguide assemblies up to the device under test are pressurized to 32 psi, except the AIRCOM phase shifter, it is pressurized to 15 psi. All high power testing was done with the pentaplate test cell shown in the frontispiece. It is surrounded by a constant temperature or cooling jacket to be used for future evaluation of the exact phase shift dependence on temperature of different materials. The picture shows the uncoated electrode configuration; in operation, the electrodes are teflon coated.

The first high power test conducted was of the phase shifter cell with the electrodes in place but using only carbon tetrachioride and without any bias voltage on the electrodes. This test was to determine possible RF breakdown in the phase shifter cell.

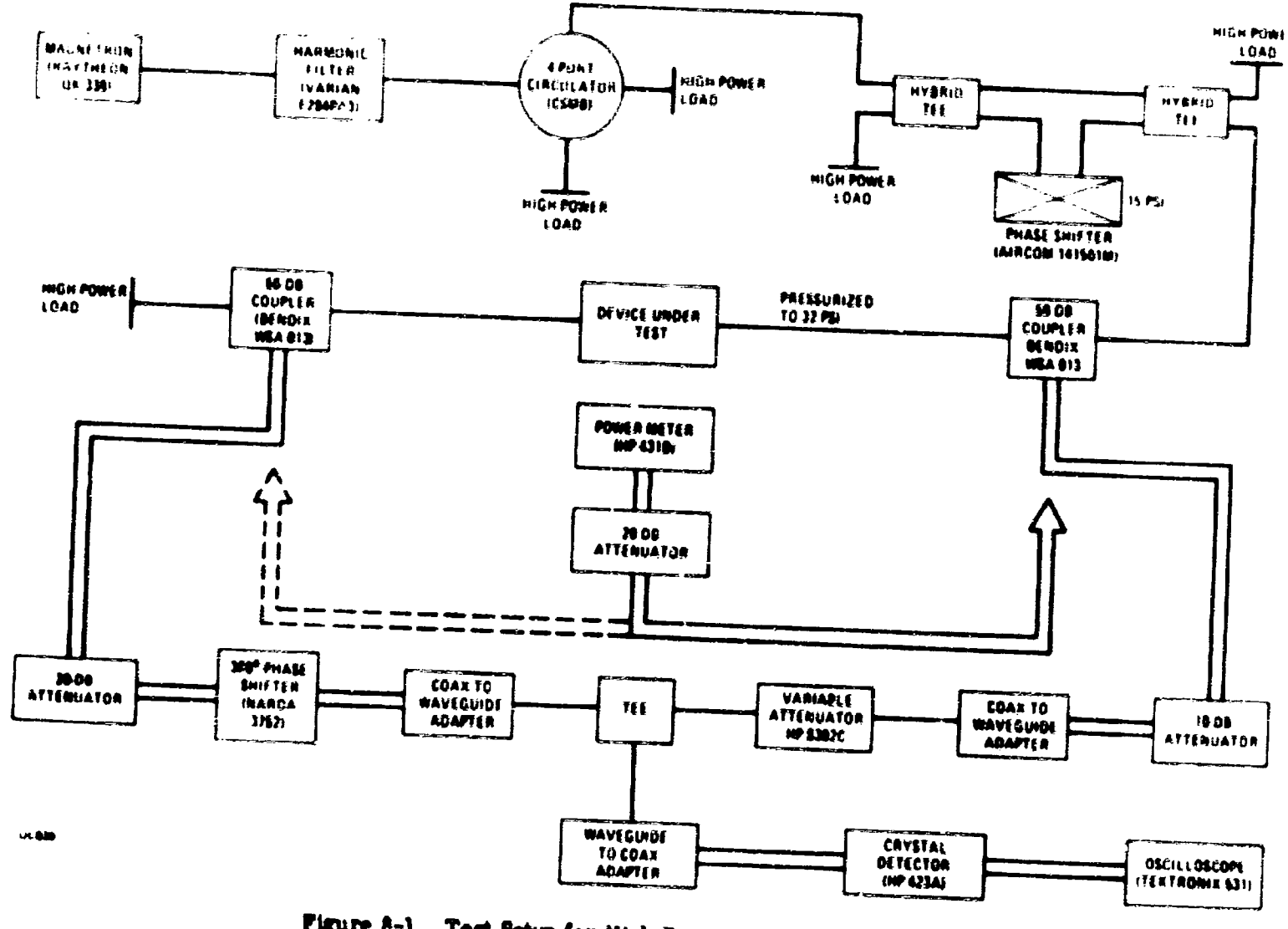

Figure 8-1. Test Setup for High Power Liquid Phase Shifter

For a rectangular waveguide operating in the TE_{10} mode the maximum power handling capability can be expressed by:

$$P = 6.63 \times 10^{-4}\, ab\left(\frac{\lambda}{\lambda_g}\right)(E_{max})^2 \qquad (8\text{-}1)$$

where:

P = Power in watts

a = Width of waveguide in cm

b = Height of waveguide in cm

λ = Free space wavelength

λ_g = Waveguide wavelength (same units as are used for λ)

E_{max} = Breakdown voltage gradient of the dielectric filling the waveguide in volts/cm

Other factors to be considered with the formula are the VSWR and internal pressure. The VSWR of the waveguide lowers the maximum power handling capability of the waveguide by the reciprocal of the magnitude of the VSWR. At higher internal pressures, the power is approximately proportional to the square of the density of air. To determine the maximum voltage between the electrodes for the rated transmitter peak power of 5 megawatts and for equal electrode spacing the following data was used:

P =	5	megawatts
a =	7.21	cm
b =	3.40	cm
λ =	10.74	cm
λ_g =	16.1	cm

Solving for E_{max} gives

$$E_{max} = \left[\frac{P\lambda_g}{6.63 \times 10^{-4}\, ab\lambda}\right]^{1/2} \text{volts/cm} \qquad (8\text{-}2)$$

Using the operating data, one obtains, for an air-filled guide at the center of the waveguide a maximum field strength, E_{max}, of 21475 volts/cm, corresponding to a peak voltage level of about 73,000 volts. The maximum voltage gradient of the waveguide with dry air is approximately 102,000 volts/cm. Therefore, a voltage breakdown of the phase shifter cell with only the electrodes in place cannot occur. The

dielectric constant of carbon tetrachloride is 2.17 at room temperature and the breakdown gradient is increased by the same factor.

The first test for RF breakdown was conducted in four steps. The respective average power levels were 263, 660, 932, and 1050 watts. The highest peak power level recorded was 1.5 megawatts. While increasing the peak power to about 2 megawatts an RF breakdown in the harmonic filter was noticed. An operating level for the filter was then established below the breakdown level. Table 8-1 shows that a peakpower level of 1.5 megawatts was the maximum possible power level for phase shifter testing.

The tests of the phase shifter cell filled with CCl_4 and the pentaplate electrode configuration in place showed that RF breakdown at a peakpower level of 1.5 megawatts and an average power level of 1050 watts is not a problem for the base solvent.

Subsequent tests were made of insertion loss as a function of carbon tetrachloride and carbon tetrabromide, see Figure 8-2. The addition of carbon tetrabromide increased the insertion loss by 0.1 dB over that of pure carbon tetrachloride. It is known that CBr_4 has a higher affinity for water and this could have produced the slight increase in insertion loss. Another potential contribution to this increase in insertion loss may be caused by polar impurities in the carbon tetrabromide because the available material was not of spectrographic quality.

Table 8-1. Harmonic Filter Operating Characteristics as a Function of Peakpower Level (Duty Cycle .0007)

Power Level		
Average (watts)	Peak (Mw)	Remarks
1050	1.500	Normal Filter Operation
1300	1.857	Irregular Filter Breakdown
1600	2.285	Consistent Filter Breakdown
1800	2.571	Consistent Filter Breakdown

NOTE: The Varian filter was supplied with a 10 megawatt peakpower rating for continuous operation.

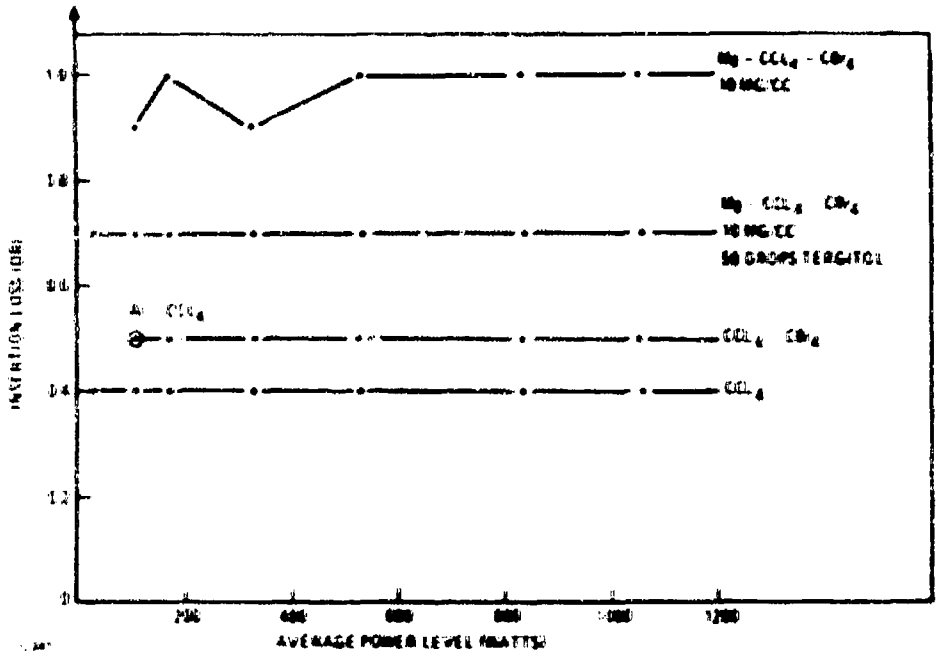

Figure 4-2. Insertion Loss vs. Average RF Power Level, at Insertion Phase Delay with no Bias Field

The next step in the test cycle was to add magnesium to the CCl_4-CBr_4 mixture. The phase shifter liquid was compounded for a maximum of 90° phase shift. This increased the phase shifter insertion loss to 1.0 dB. The phase shift data in Figure 4-3 has been obtained with this material. Electrode breakdown occurred at the high applied voltage levels and the higher RF power levels.

After completion of all tests the electrodes were removed for inspection to determine the cause of breakdown. The apparent cause is attributed to insufficient teflon coating for about 3 in. on one of the edges of the electrode. The region of arcing, which is the cause of the breakdown, is only the edge of one electrode located closest to the waveguide housing, Figure 4-4a. Arcing started from the electrode edge in the teflon support along the teflon support to the waveguide housing, Figure 4-4b. Also shown is the observed thin portion of the teflon coated edge of the electrode. The actual onset of arcing can be seen to be the six corners of the electrode, Figure 4-4c. These are material points of high field intensity where arcing would be expected to start.

Another set of phase shift data was taken after the addition of 50 drops of the surfactant Tergitol. The important properties of surfactants, shown in Figure 4-5, was the addition of Tergitol, which reduced the insertion loss characteristics to 0.1 dB

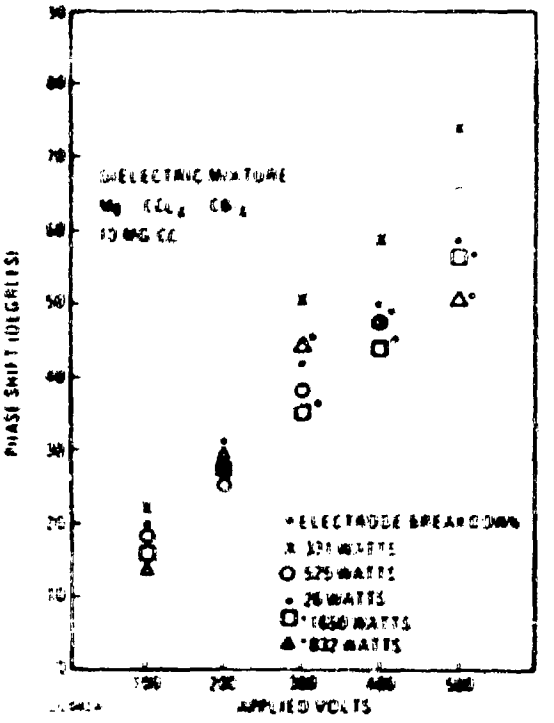

Figure 6-3. Phase Shift vs. Applied Voltage for Various Power Levels

and, in Figure 6-5, where the amount of phase shift obtained for a given applied voltage is increased over that obtained from the Mg-CCl_4-CBr_4 dielectric only. The advantage of adding a surfactant is shown in Figure 6-6. This is the first time that the merits of adding surfactants have been shown clearly. Previous work was primarily concerned with keeping the mixture of the liquid dielectric as simple as possible.

This is a very important result in the sense that it appears possible to allow even further reduction of phase shifter insertion loss in the aluminum-carbon tetrachloride dielectric which has an insertion loss of only one half that of Mg-CCl_4-CBr_4 or 0.5 dB maximum, although aluminum-based artificial dielectrics of large particle size would have to be pumped. This consideration makes it even more important to exploit the use of extremely small particles.

Limited measurements of the change in insertion loss as a function of phase shift was made at average power levels of 331 and 525 watts. The results, Figure 6-7, indicate an increase of insertion loss by 0.5 dB.

The last high power test performed was that of determining any relative phase shift as a function of power level, see Figure 6-8. Considering instrumentation errors one must conclude that there is no definite change in phase shift as a function of RF average power levels up to one kilowatt, as tested. This is in a real sense a reassuring result, inasmuch as it indicates that RF interaction with the particles does not seem to take

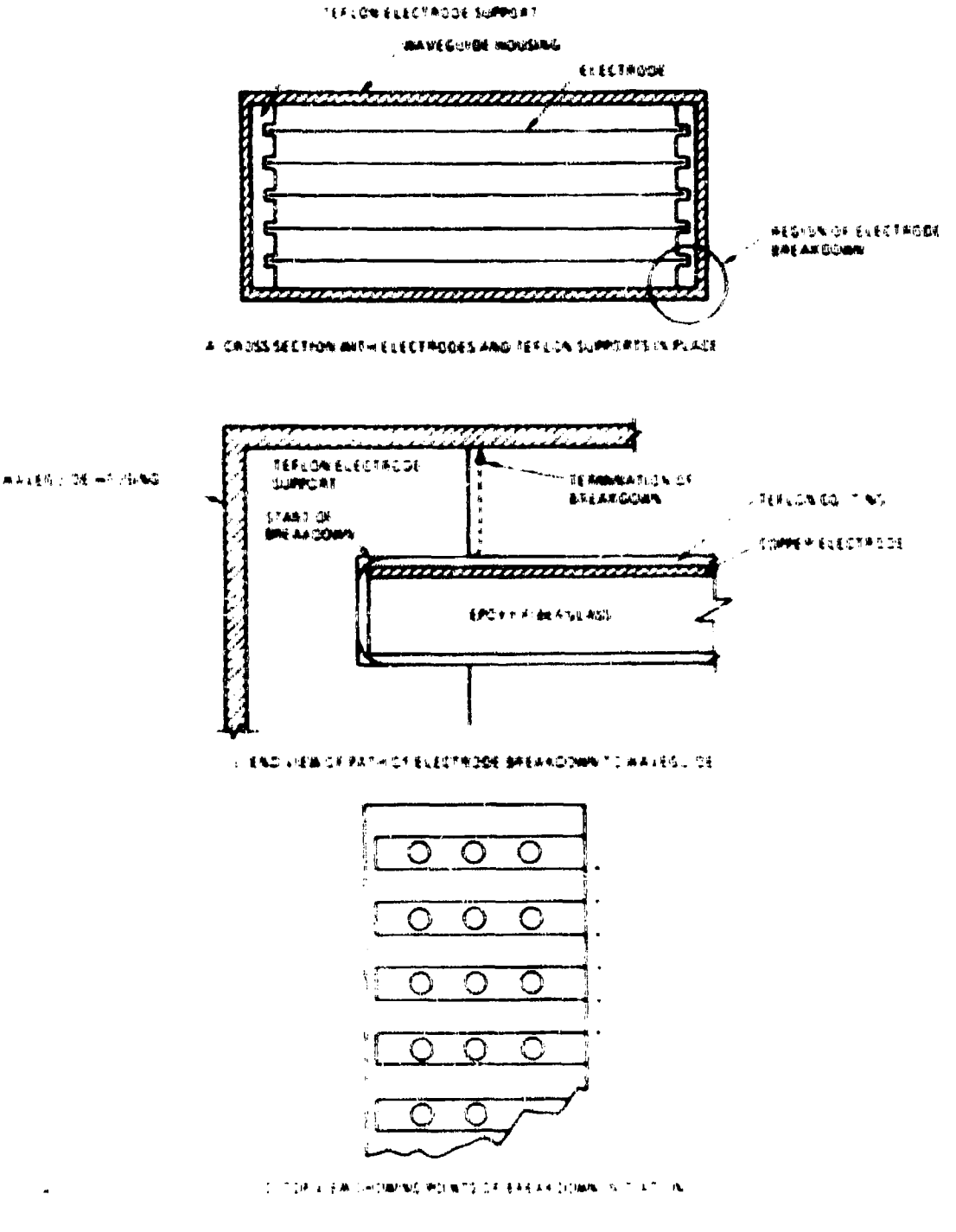

Figure 7-4. Phase Shifter Cell Electrode Breakdown Caused by Insufficient Electrode Coating

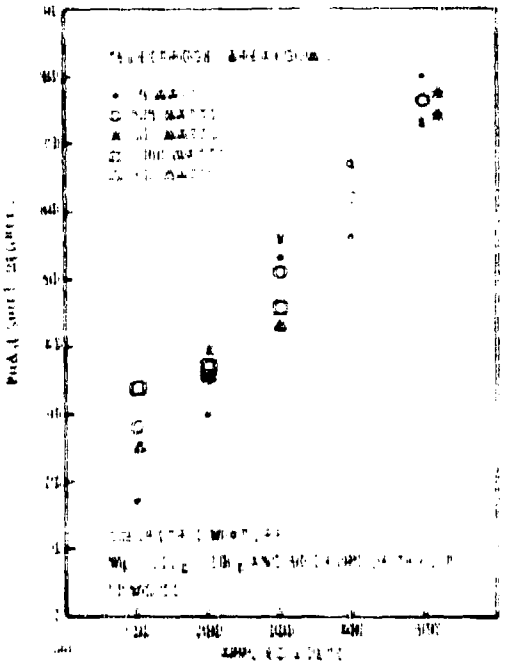

Figure 4-5. Phase Shift vs. Applied Voltage for Various Power Levels After Adding Tergitol

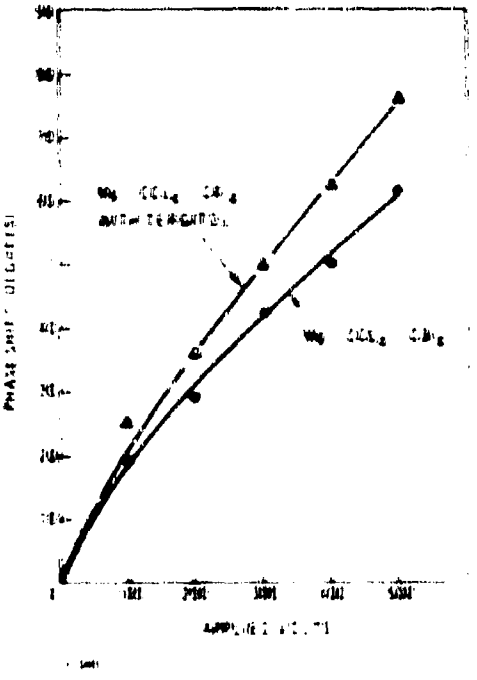

Figure 4-6. Increase of Phase Shift After Surfactant Added to Dielectric

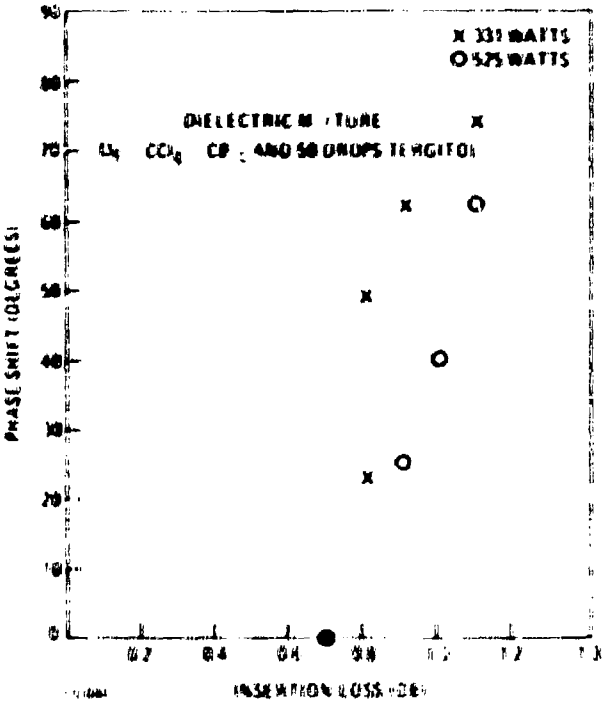

Figure [illegible]. Change of Insertion Loss as a Function of Phase Shift

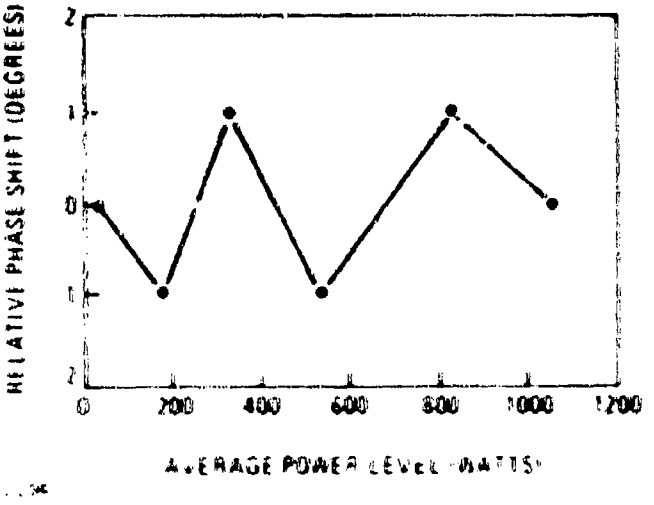

Figure [illegible]. Relative Phase Shift vs. Power Level, at Insertion Phase Delay

place, although a firm conclusion to that effect cannot be drawn from the limited experimental data.

After tests with the magnesium based dielectric were completed, a mixture of aluminum and carbon tetrachloride was put into the test cell. Only limited tests could be run since prolonged electrode arcing at high applied voltages had established a low level of breakdown. The Al-CCl_4 liquid exhibited breakdown at 166 watts average, see Table 8-2. This problem was related to electrode arcing caused by aluminum coating action, although this could not be verified from subsequent inspection of the waveguide housing and the electrode assembly. The results demonstrate rather forcefully the reduction of obtainable phase shift when the liquid is rapidly pumped through the cell. It appears that particle alignment by this bias field is quite limited. The effect is similar to that of Brownian motion itself, where particles are kept in random orientation and even limited orientation requires a certain threshold voltage to overcome the effects of Brownian motion.

Table 8-2. Al-CCl_4 Phase Shift Tests

(Power Level: 105 Watts Average)

Applied Voltage (Volts)	Phase Shift		Insertion Loss	
	Pump On (Deg.)	Pump Off (Deg.)	Pump On (dB)	Pump Off (dB)
0	0°	0°	0.5	0.5
167	45°	193°	0.6	Electrode Arcing*

*The same set of electrodes were used for the entire testing phase.

9. SUMMARY AND CONCLUSIONS

Analytical and experimental studies were concerned with establishing the feasibility of developing a reciprocal, high power, analog phase shifter applying the principles of electrically controllable liquid artificial dielectrics.

The particular areas investigated were: phase shift cell design; electrode coating, pumping system, metallic suspensions; proteins, and liquid crystals. Low power measurements of insertion loss, VSWR, phase shift, and response time were made to describe the phase shifter performance. Subsequent to establishing a high power facility capable of providing a peak power of 5 megawatts at an average power level of 3.6 kilowatts a series of high power tests were made with a magnesium based artificial dielectric compounded for a phase shift of 90° at a saturation voltage of approximately 500 volts. The device was tested to 1.5 MW peak power and 1 kW average. Some dependence of the breakdown voltage and the power of the microwave field was observed.

Two phase shifter electrode designs were evaluated by insertion loss and VSWR measurements over the band of frequencies from 2.7 to 2.9 GHz. The insertion loss due to electrode configuration is reduced by increasing the hole size in the electrode. This tends to equalize the flow characteristics. It was also observed that the edge of the single electrode generated higher order modes. A TE_{20} mode field was measured at the discontinuity and in the region of the electrode. The best results, however, were obtained with a five-plate electrode configuration. All insertion loss peaks were eliminated, no moding was observed, and it has the advantage of providing higher field intensity with low applied control voltage. Although the present pentaplate design may not be optimum, it certainly demonstrates that avenues for optimization are available.

All electrodes used are teflon coated to reduce potential breakdown problems, however, the results from high power testing indicated that the edges of the electrodes should be coated carefully, because the coating at the edges is usually much thinner than on the flat portion. The need for teflon coating may, however, be eliminated altogether by using a metallic suspension of coated particles that do not paint.

The pumping system was used during early experiments to agitate the suspension and prevent the particles from settling out. A thorough study of the pumping requirement and its effects on phase shift performance was made with the conclusion that moving the liquid reduces the available phase shift by as much as 5% as demonstrated during high power tests with the Al-CCl_4 system. This is true for both laminar and turbulent flow. This strongly supports the preferred direction of phase shifter development because elimination of the pumping system was an early goal, to keep the phase shifter design as simple and cost effective as possible.

Of all the liquid systems tested the aluminum-carbon tetrachloride dielectric provided the greatest phase shift, — 1000° at Ku for 200 volts rms without pumping; however, the particle size is quite large and therefore intermittent pumping would be required to prevent particle settling. Beyond that it appears that aluminum does have a tendency to paint the electrode support surfaces thus contributing to eventual breakdown.

To eliminate the need for a pumping system a new dielectric system was developed consisting of magnesium, carbon tetrachloride, and carbon tetrabromide. Both liquids are mixed in a proportion to match the density of the liquid to that of the magnesium particles. This density-matched system is now stable in suspension, at least for 2 months and does not require pumping. At the present time the amount of obtainable phase shift is only about 50% of aluminum. This is caused by the large particle size (10-20 microns). Thus a given particle weight density has a much lower particle number density, hence the reduced obtainable phase shift. The density-matched system is also stable over a range of temperatures from about 15° to 40°C.

Magnesium particles tended to flocculate; some experiments indicated that this could be caused by water. This problem was solved by adding a surfactant Tergitol. It provided two additional benefits. Insertion loss of the $Mg-CCl_4-CBr_4$ was reduced from 1 dB to 0.7 dB and phase shift properties were increased for a 90° test cell.

Liquid crystals were also studied at Ku-band in an effort to find a one-component system. The nematic liquid crystals had a very high insertion loss. The cholesteric types showed no absorption at Ku-band; however, it appeared that the duty cycle of the Cober high voltage power supply was not high enough to observe appreciable amounts of phase shift. Five solutions of liquid crystals in hexane or carbon tetrachloride yielded no observable phase shift. These may also require higher voltages with high duty cycle or even dc because liquid crystals generally tend to require high applied electric fields when used for displays.

Proteins were examined for use as one-component artificial dielectrics because of their large dipole moments. Since all of them are only soluble in either water or ethanol, they do have high absorption in the microwave region and are therefore not useful.

The effort to use lowest possible applied voltage for 360° phase shift with particles in the size range of 5 to 25 microns does not produce fast response times. As predicted by the theory and verified by measurements the response time for particles with an average diameter of about 10 microns and for an applied voltage of 100 volts, the response time is about 1 sec. Since according to theory the response time depends on the third power of the particle radius and approximately on the second

power of the applied field, two data points verifying the theory have been obtained. One data point was obtained by Buscher (7) in 1972 in which the particles were reduced in size by one order of magnitude by ballmilling them for three days and by applying a field of 20 kV to obtain a phase shift of 360°, thereby observing a response time of 10 microseconds. As the theory shows, the strongest dependence for fast response times is on particle size. This appears to be the preferred direction of liquid phase shifter development since it does not require the use of high voltages. However, high voltages do increase the potential for breakdown.

The response time behavior of small and large particles in suspension is theoretically quite well understood. From our investigations it appears that a theory to accurately predict response time behavior of large particles for very high field strength is not yet fully developed.

The high power tests, although very successful, were limited to a peak power level of 1.5 megawatts and an average power level of 1050 watts. This limitation was imposed by breakdown by the harmonic filter at less than 2 megawatts. After approximately one week of testing, electrode breakdown by arcing was observed. Inspection showed that arcing started from a corner of one electrode nearest the waveguide housing and was caused by the insufficient thickness of teflon coating on the edges.

From the analytical and experimental results obtained on this program it can be concluded that the existing theory for metallic particle suspension has been verified at two extreme points of response time providing a solid base of what can be expected in future work. Although the results were obtained at different frequencies the implications concerning response time are still valid. The results also indicate that, for fast response time needs, small particles are desired. Moreover, they also remain a stable suspension indefinitely.

Liquid density matching techniques are very useful but as a rule they operate over a limited range of temperatures. (A suspension of Mg CCl_4 CBr_4 is stable for at least two months.) The particles in the presently used suspension tend to rise at 15°C and settle at about 40°C. whether this range of temperature can be widened is at present doubtful. The importance of the use of surfactants for reducing insertion loss and increasing available phase shift is also demonstrated and should be exploited to full advantage. Several problem areas have been highlighted in view of the results obtained and they point the way for obtaining better performance characteristics.

It can be concluded that the approach seems feasible for developing a reciprocal, high power, low loss, analog phase shifter both simple in construction and low cost in even small quantities. Direction for future work to optimize specific performance characteristics has been shown.

10. BIBLIOGRAPHY

1. Condon, E. V. & Odishaw, H., Handbook of Physics, McGraw-Hill Book Company, N.Y. 1958 p. 6-120

2. Encyclopedia of Polymer Science and Technology, Vol. 9 p. 553

3. Collin, R. E., Field Theory of Guided Waves, McGraw-Hill Book Company., N.Y. 1960, p. 512

4. O'Konski, C.T., Molecular Electro-Optics, O'Konski, C.T., ed, Marcel Dekker Inc., N.Y., N.Y. (To be published) Chapter 3 (The authors wish to thank Professor O'Konski for the use of this material before publishing.)

5. Böttcher, C. J. F., Theory of Electric Polarization, Elsevier Amsterdam (1954)

6. Frenkel, J., Kinetic Theory of Liquids, Dover, N.Y. N.Y. (1955) p. 205

7. Development of High Power Phased Arrays, GDE Report R-72-035

8. O'Konski, C. T., and Zimm, B. H. Science, 3, 113 (1950)

9. Benoit, H., Amer Phys., 6 561 (1951)

10. Southworth, G. C., Principles and Applications of Waveguide Transmission, D. Van Nostrand Company, Inc., 1950

11. Eskinazi, S., Principles of Fluid Mechanics, Allyn and Bacon, Inc., Boston, 1962 p. 362

12. Reference 11, p. 395

13. Reference 1, p. 6-124

14. Reference 7

15. Minford, J. D., et. al., J. Electrochem Soc., 106, 185 (1959)

16. Watanabi, H., et. al., Biopolymers, 2, 91 1964

17. Meier, G., and Saupe, A., Liquid Crystals., Gordon & Breach, N.Y., 1967

18. McClellan, A. L., Tables of Experimental Dipole Moments, Freeman, San Francisco, p. 63

19. Reference 4